การสังเคราะห์อนุพันธ์เฟอร์โรซีนที่มีตัวรับแบบต่างๆ เพื่อเป็นตัวรับรู้ไซยาไนด์ไอออน

นางสาวอรวรรณ วิเศษสุนทร

วิทยานิพนธ์นี้เป็นส่วนหนึ่งของการศึกษาตามหลักสูตรปริญญาวิทยาศาสตรมหาบัณฑิต
สาขาวิชาเคมี ภาควิชาเคมี
คณะวิทยาศาสตร์ จุฬาลงกรณ์มหาวิทยาลัย
ปีการศึกษา 2559

SYNTHESIS OF FERROCENE DERIVATIVES CONTAINING VARIOUS RECEPTORS AS CYANIDE ION SENSORS

Miss Orrawan Wisedsoonthorn

A Thesis Submitted in Partial Fulfillment of the Requirements
for the Degree of Master of Science Program in Chemistry
Department of Chemistry
Faculty of Science
Chulalongkorn University
Academic Year 2016

Thesis Title	SYNTHESIS OF FERROCENE DERIVATIVES CONTAINING VARIOUS RECEPTORS AS CYANIDE ION SENSORS
By	Miss Orrawan Wisedsoonthorn
Field of Study	Chemistry
Thesis Advisor	Professor Thawatchai Tuntulani, Ph.D.

Accepted by the Faculty of Science, Chulalongkorn University in Partial Fulfillment of the Requirements for the Master's Degree

.....Dean of the Faculty of Science
(Associate Professor Polkit Sangvanich, Ph.D.)

THESIS COMMITTEE

.....Chairman
(Associate Professor Vudhichai Parasuk, Ph.D.)

.....Thesis Advisor
(Professor Thawatchai Tuntulani, Ph.D.)

.....Examiner
(Professor Vithaya Ruangpornvisuti, Dr.rer.nat.)

.....Examiner
(Associate Professor Nuanphun Chantarasiri, Ph.D.)

.....External Examiner
(Assistant Professor Chomchai Suksai, Ph.D.)

อรวรรณ วิเศษสุนทร : การสังเคราะห์อนุพันธ์เฟอร์โรซีนที่มีตัวรับแบบต่างๆ เพื่อเป็นตัวรับรู้ไซยาไนด์ไอออน (SYNTHESIS OF FERROCENE DERIVATIVES CONTAINING VARIOUS RECEPTORS AS CYANIDE ION SENSORS) อ.ที่ปรึกษาวิทยานิพนธ์หลัก: ศ. ดร.ธวัชชัย ตันฑุลานิ, 65 หน้า.

งานวิจัยนี้มีจุดประสงค์ในการออกแบบและสังเคราะห์โมเลกุลเซ็นเซอร์ สำหรับใช้ในการตรวจวัดไซยาไนด์แอนไอออน โดยมีแอริลอีไทน์เป็นตัวเชื่อมระหว่างหมู่ที่ให้สัญญาณกับหมู่ที่เป็นรีเซ็ปเตอร์ผ่านปฏิกิริยาโซโนกาชิราคัปปลิง ได้ทำการสังเคราะห์อนุพันธ์ของเฟอร์โรซีนแบบอสมมาตรที่ประกอบด้วยกรดโบโรนิก และ ไดพิโคลิลเอมีนเป็นรีเซ็ปเตอร์ L1 และ L2 มีปริมาณผลิตภัณฑ์ร้อยละ 45 และ 67 ตามลำดับ เมื่อศึกษาการเปลี่ยนแปลงของสัญญาณรีดอกซ์ของเฟอร์โรซีนของ L1 ใน 0.1 M $TBAPF_6$ ในแอซีโตไนไตรล์ พบว่ามีความจำเพาะอย่างสูงกับไซยาไนด์เมื่อเทียบกับแอนไอออนตัวอื่นๆ นอกจากนี้ยังศึกษาการเกิดอันตรกิริยาระหว่าง L1 ในเมทานอลกับไซยาไนด์โดยวิธี ^1H NMR ไทเทรชัน พบว่าไซยาไนด์สามารถเข้าไปจับที่บริเวณโบรอนอะตอมของกรดโบโรนิก สำหรับ L2 เมื่อศึกษาด้วยไซคลิกโวลแทมเมทรีกับไอออนของโลหะต่างๆ ใน 0.1 M $TBAPF_6$ ในสารละลายผสม 10% ไดคลอโรมีเทนในแอซีโตไนไตรล์ พบว่า L2 สามารถเกิดอันตรกิริยากับคอปเปอร์ไอออนได้ดีที่สุด โดยเกิดการเปลี่ยนแปลงสัญญาณรีดอกซ์ของเฟอร์โรซีน และปรากฏสัญญาณรีดอกซ์ของคอปเปอร์ เมื่อศึกษาด้วยยูวี วิซิเบิลสเปกโทรโฟโทเมทรีในแอซีโตไนไตรล์ พบว่าเกิดการเปลี่ยนแปลงค่าความยาวคลื่นจาก 310 ไปยัง 260 นาโนเมตร จึงยืนยันได้ว่า L2 สามารถเกิดอันตรกิริยากับคอปเปอร์ได้ดีและเมื่อศึกษายูวี วิซิเบิลสเปกโทรโฟโทเมทรีของ L2-Cu^{2+} กับแอนไอออนต่างๆ พบว่ามีเพียง CN^-, $H_2PO_4^-$ และ F^- ส่งผลให้เกิดการเปลี่ยนแปลงค่าความยาวคลื่นจาก 260 กลับมายัง 310 นาโนเมตร เมื่อศึกษาด้วยไซคลิกโวลแทมเมทรีของ L2-Cu^{2+} กับ CN^- และ F^- ใน 0.1 M $TBAPF_6$ ใน สารละลายผสม 10% ไดคลอโรมีเทนในแอซีโตไนไตรล์ พบว่าไม่เกิดการเปลี่ยนแปลงสัญญาณรีดอกซ์ของเฟอร์โรซีน และในขณะเดียวกันสัญญาณรีดอกซ์ของคอปเปอร์หายไปด้วย จึงคาดว่า CN^- และ F^- สามารถเข้าไปเกิดอันตรกิริยากับคอปเปอร์ใน L2-Cu^{2+} สำหรับ $H_2PO_4^-$ พบการตกตะกอนระหว่างการทดลอง จึงไม่สามารถตรวจวัด $H_2PO_4^-$ ด้วยไซคลิกโวลแทมเมทรีได้

ภาควิชา เคมี ลายมือชื่อนิสิต .....

สาขาวิชา เคมี ลายมือชื่อ อ.ที่ปรึกษาหลัก .....

ปีการศึกษา 2559

5772211023 : MAJOR CHEMISTRY

KEYWORDS: FERROCENE / BORONIC ACID / DIPICOLYLAMINE / CYANIDE / ELECTROCHEMICAL

ORRAWAN WISEDSOONTHORN: SYNTHESIS OF FERROCENE DERIVATIVES CONTAINING VARIOUS RECEPTORS AS CYANIDE ION SENSORS. ADVISOR: PROF. THAWATCHAI TUNTULANI, Ph.D., 65 pp.

The goal of this research is to design and synthesize molecular sensor for cyanide anion. The signalling unit and receptor unit were connected through aryl ethyne moiety by using Sonogashira-cross coupling. The unsymmetrically ferrocene derivatives containing boronic acid and 2, 2-dipicolylamine (DPA) as receptor unit, L1 and L2, were obtained in moderate yields, 45% and 67%, respectively. Cyclic voltammetry of L1 in 0.1 M $TBAPF_6$ in CH_3CN exhibited high selectivity toward cyanide ions in the presence of various anions. In addition, the binding of cyanide at the boron center of L1 was supported by ^1H NMR titrations of L1 and cyanide ions in CD_3OD. The cyclic voltammetry studies of L2 with various metal ions in 0.1 M $TBAPF_6$ in CH_3CN exhibited high selectivity toward Cu^{2+} ion. The cyclic voltammogram of L2-Cu^{2+} showed the shift of the redox potential of ferrocene and a reversible redox wave of Cu^{II}/Cu^{I}. The blue-shift of absorption spectrum from 310 to 260 nm in UV-Vis spectrum of L2 upon addition of Cu^{2+} supported the result from cyclic voltammetry. In the presence of CN^-, $H_2PO_4^-$ and F^-, the UV-Vis spectrum of L2-Cu^{2+} exhibited a red shift of the absorption band from 260 to 310 nm. Using cyclic voltammetry, the addition of CN^- or F^- to the solution of L2-Cu^{2+} complex in 0.1 M $TBAPF_6$ in CH_3CN did not show any potential shift of the Fc/Fc^+ redox couple. In addition, the reversible wave of Cu^{II}/Cu^{I} redox couple disappeared, indicating that CN^- and F^- interacted at the copper (II) center of L2-Cu^{2+} complex. Addition of $H_2PO_4^-$ to the solution of L2-Cu^{2+} complex resulted in the precipitation. Therefore, L2-Cu^{2+} complex cannot be used for detection of $H_2PO_4^-$ by cyclic voltammetry.

Department: Chemistry Student's Signature .....

Field of Study: Chemistry Advisor's Signature .....

Academic Year: 2016

ACKNOWLEDGEMENTS

I would like to thank my research advisor, Professor Dr.Thawatchai Tuntulani, for his invaluable guidance and helpful suggestions throughout this research and the opportunity to work in this great research unit. In addition, I would like to thank and pay my respect to Associate Professor Dr.Vudhichai Parasuk, Professor Dr.Vithaya Ruangpornvisuti, Associate Professor Dr.Nuanphun Chantarasiri and Assistant Professor Dr.Chomchai Suksai for their valuable advices and comments as thesis committee.

Furthermore, I would like to thank the Thailand Research Fund (RTA5380003) for financial support. I greatfully thank all member of Supramolecular Chemistry Research Unit at the department of Chemistry Chulalongkorn University for their support.

Finally, I would like to thank all members of my family for their love, care, kindness, encouragement and financial support throughout my life.

CONTENTS

Page

Page

Page

LIST OF SCHEMES

LIST OF FIGURES

LIST OF TABLES

LIST OF ABBREVIATIONS AND SYMBOLS

Calcd.	Calculated
δ	Chemical shift
^{13}C NMR	Carbon-13 nuclear magnetic resonance
CH_2Cl_2	Dichloromethane
CH_3CN	Acetonitrile
CV	Cyclic voltammetry
EtOAc	Ethylacetate
equiv.	equivalent
g	gram
^{1}H NMR	proton nuclear magnetic resonance
h	hour
Hz	Hertz
J	coupling constant
m/z	mass per charge ratio
µL	microliter
µM	micromolar
M	molar
mg	milligram
min	minute
mL	milliliter
mmol	millimole
mV/s	millivolt per second
NEt_3	triethylamine
ppm	part per million
Pt	platinum

rt	room temperature
s, d, t, m	splitting pattern of ^{1}H NMR (singlet, doublet, triplet, multiplet)
UV-Vis	Ultraviolet Visible
DFT	Density Functional Theory

CHAPTER I

INTRODUCTION

Recently, recognition and detection of anions has become an interesting field of research because anions play important roles in many fields such as catalysis, medicine, biological and environmental sciences. Cyanide is produced in large qualities from different industrial applications, including polymer synthesis, metallurgy and mining [1-4]. Therefore, cyanide can be released in a widespread way from industrial uses. In addition, cyanide was found to cause irritation, pain and nervous instability. For these reasons, it is necessary to detect and remove this dangerous anion either from industrial waste water or an accidental release. Thus, the development of methods or techniques to detect cyanide has become a topic of interest.

The detection of cyanide can be successfully carried out by using supramolecular chemistry–based molecular sensors. This method is selective, comfortable and inexpensive [5, 6]. Therefore, the design of synthetic receptors for cyanide complexing and sensing has been a great challenge.

1.1 Organoborane-based anion receptor

1.1.1 Boron-anion interactions

Trisubstituted boron atoms have a sp^2 trigonal planar geometry with an empty p orbital. Nucleophiles interact with or donate electron density to the vacant site, resulting in a change of geometry from trigonal planar to tetrahedral (**Scheme 1.1**) [7]. The studies about the interactions between boronic acids and anions were first reported in 1959 by Lorand and Edwards [8].

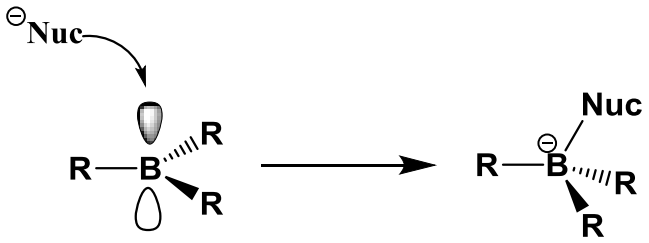

Scheme 1.1 Change in geometry at the boron center when the vacant p orbital is filled by an attacking nucleophile [7].

In particular, the boron atom which acts as a Lewis acidic was used as a receptor for anions such as fluoride, hydroxide and cyanide.

1.1.2 Anion receptors based on organoborane

In 1995, Dusemund and coworkers [9] reported the electrochemical detection of fluoride ions with Lewis acid boron in aqueous solution. In this research, the boronic acid receptor unit was connected to a ferrocene redox-signaling unit (**1**). Results suggested that the F^--binding event occurred at the boronic acid site due to the shift of the redox potential of the ferrocene moiety as shown in **Figure 1.1**.

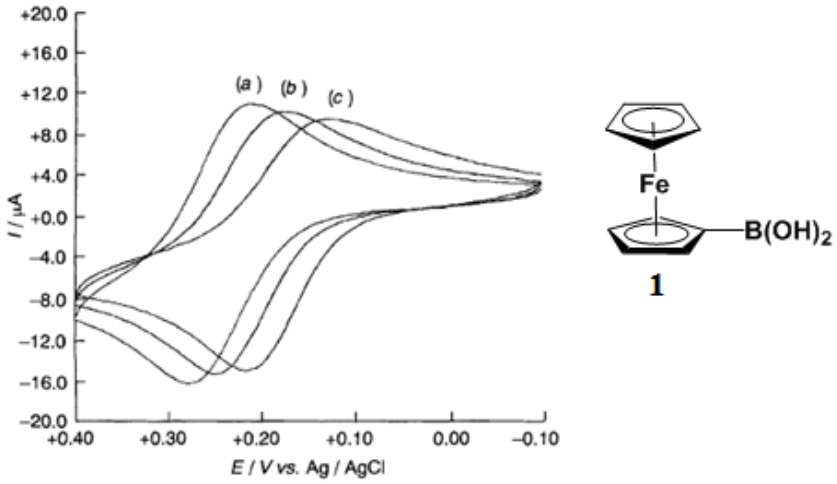

Figure 1.1 Cyclic voltammograms of **1** at a glassy carbon electrode [0.5 mM $FcB(OH)_2$, 0.1 M $NaClO_4$], with varying concentrations of F^-, v = 500 mV s^{-1}; (a) $[F^-]$ = 0; (b) $[F^-]$ = 9.1×10^{-3} M; (c) $[F^-]$ = 4.5×10^{-2} M [9].

The strong electron-withdrawing ability of the ferrocenium moiety creates an electron-deficient boron center. Therefore, a better interaction with fluoride ions is expected. The oxidized species of **1** has a stronger interaction with fluoride ions compared to the neutral boronic acid, the main redox reaction is expressed by equation **(1)**.

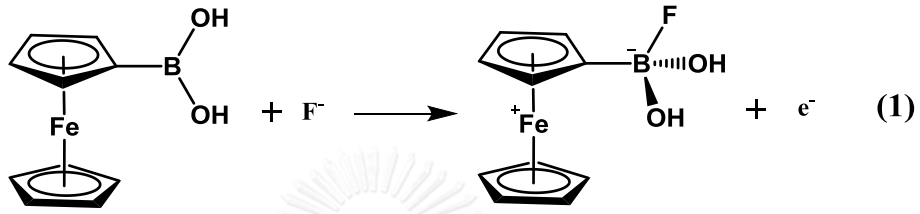

In 2006, Swamy and coworkers [10] reported a new fluorescein derivative (**2**) that displays a selective fluorescent changes with fluoride ion among halide ions. The fluorescent changes were due to a photo-induced electron transfer (PET) mechanism induced by the interaction between fluoride and the boronic acid moiety. Upon the addition of fluoride ion, the phenolic hydrogen can make a strong hydrogen bond with fluoride as well as benzylic amine, which blocks the PET mechanism (**Scheme 1.2**), resulting in a fluorescence enhancement as shown in **Figure 1.2**.

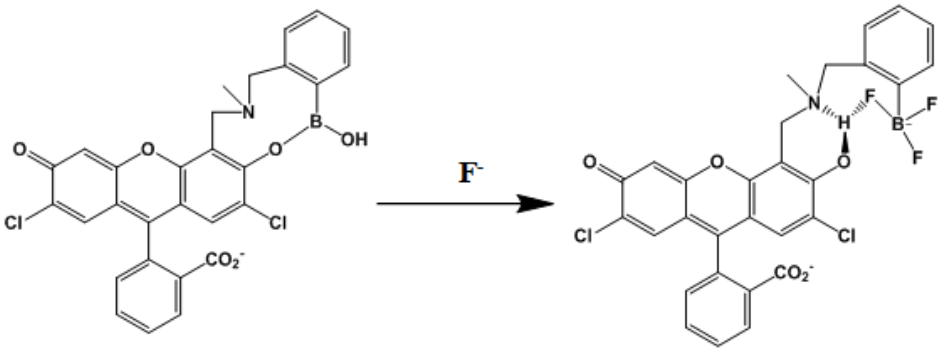

Scheme 1.2 Proposed binding mechanism of **2** with fluoride ion [10].

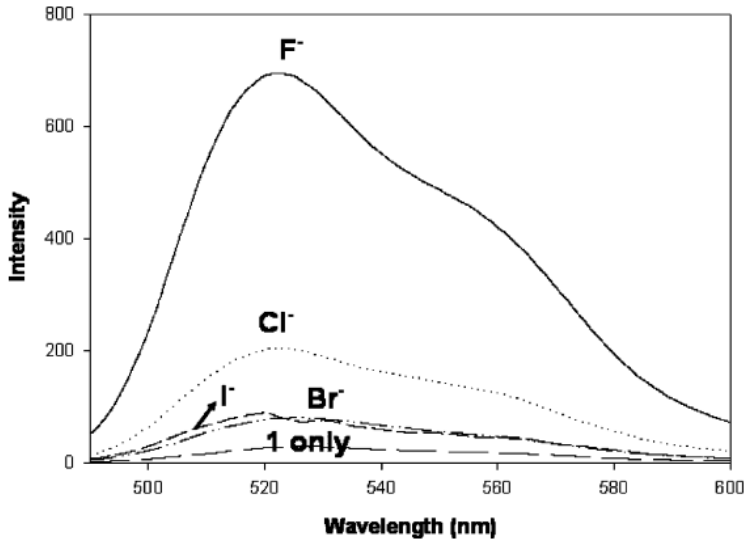

Figure 1.2 Fluorescent emission changes of **2** (3 μM) upon the addition of tetraethylammonium F^-, Br^-, Cl^- and I^- (300 equiv.) in CH_3CN-MeOH (9:1, v/v) (excitation at 483 nm) [10].

In 2001, Yamaguchi and co-workers [11] reported boron-containing π-conjugated compounds **3a**–**3d** (**Figure 1.3**) that showed a visible color change upon fluoride binding in THF. The highly conjugated system is disrupted by the boron–fluoride interaction and hybridization change of the boron from sp^2 to sp^3. This change can be explained as a result of the interruption of the π-conjugation through the formation of the corresponding fluoroborate as shown in **Scheme 1.3**.

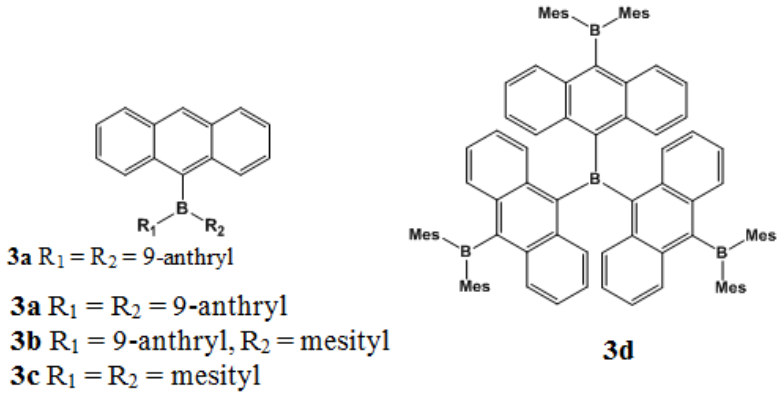

3a $R_1 = R_2 = 9$-anthryl
3b $R_1 = 9$-anthryl, $R_2 =$ mesityl
3c $R_1 = R_2 =$ mesityl

Figure 1.3 Triaryl borane species can act as colorimetric fluoride sensors [11].

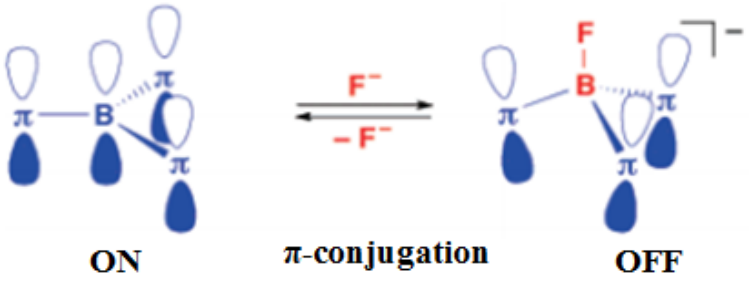

Scheme 1.3 Representation of the switching of π-conjugation in the LUMO of boron-based π-electron systems: π stands for π-conjugated moieties [11].

In 2014 Ooyama and co-workers [12] created highly-sensitive fluorescence PET sensor for a trace amount of water in various solvents. They designed and synthesized anthracene–boronic acid ester (**4**) having a methoxy group as an electron-donating substituent and a cyano group as an electron-withdrawing substituent, respectively, at the para position on benzeneboronic acid ester. This work indicates that the electron-withdrawing substituent on the benzeneboronic acid ester can enhance the Lewis acidity of the boron atom, effectively leading to formation of fluorescent ionic structure by addition of water as shown in **Scheme 1.4**.

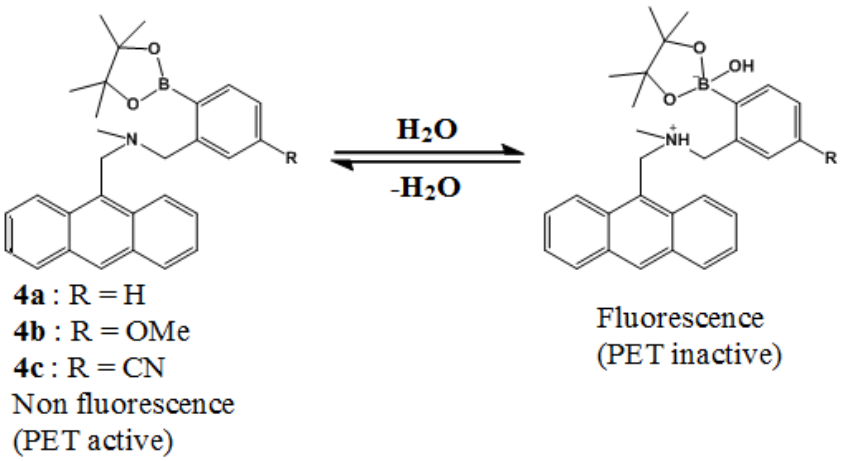

Scheme 1.4 Fluorescence PET sensors **4a**-**4c** for detection of water in organic solvents [12].

In 2011 Kim and co-workers [13] synthesized para-phenylene phosphonium borane ([**5a**]$^+$ and [**5b**]$^+$), which behave as highly sensitive fluorescence turn-on sensors for the cyanide anion in aqueous solutions. They have demonstrated that cyanide binding to the boron center of [**5a**]$^+$ and [**5b**]$^+$ results in a turn-on fluorescence of the anthryl and dansyl fluorophores, respectively, as shown in **Scheme 1.5**. The fluorescence enhancement can be explained by considering 1) that the fluorophores of [**5a**]$^+$ and [**5b**]$^+$ are quenched by intramolecular PET from the fluorophore to the electron-deficient phosphonium borane unit and 2) that cyanide coordination to the boron center neutralizes the electron accepting properties of the phosphonium borane unit leading to a revival of the fluorescence of the pendant fluorophore. The success of this approach is illustrated by the use of [**5b**]$^+$ for the naked-eye detection of cyanide ions at 50 ppb in aqueous solutions.

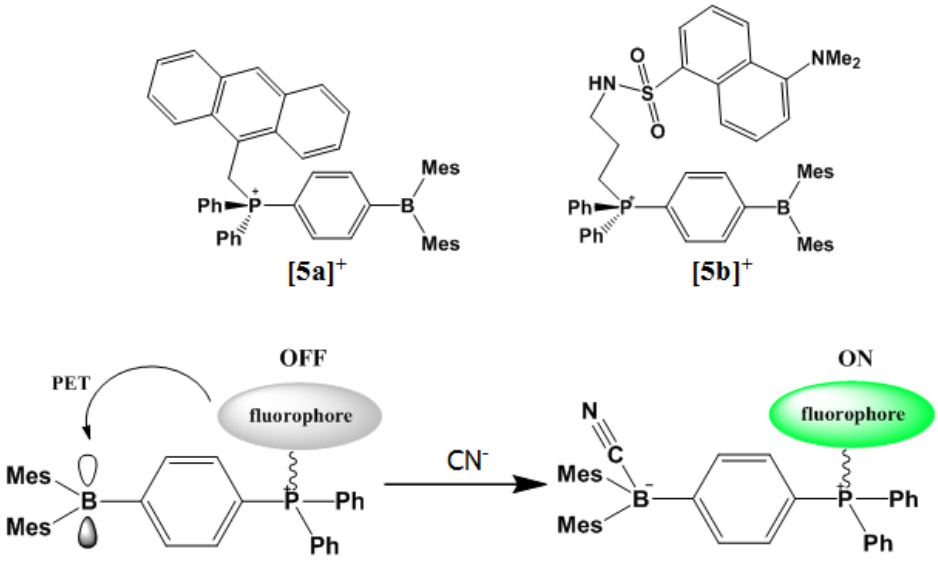

Scheme 1.5 Proposed mechanism of fluorescence quenching and revival in [**5a**]$^+$ and [**5b**]$^+$/fluorophore conjugates (PET) [13].

In 2012 Tirfoin and co-workers [14] designed the indenylferrocene functionalized borane (**6**), which is available in two simple steps from organic precursors. **6** binds cyanide in protic media (1:1, THF:H_2O) with an accompanying green to red/pink color change as shown in **Figure 1.4**. They hypothesized that a steric of metallocene functionalized borane might display a workable selectivity for CN^-. Remarkably, the extended conjugation of the indenyl backbone in **6** and the reporter chromophore make for very convenient detection of cyanide by colorimetric measurement. High selectivity over fluoride and hydroxide and a detection limit of 10 ppm represents a highly desirable combination among borane derived cyanide receptors.

Figure 1.4 The receptor **6** binds CN^- in protic media signalled by a green to red/pink color change [14].

1.2 Metal-based anion receptors

In general, metal ions in the form of organometallic and coordination complexes can be used as anion sensors. Over the last 15 years, many examples of metal-based anion sensors have been reported [4, 15-19]. Anion receptors based on metal center is most commonly incorporated as a reporter group including photochemical or electrochemical response, mainly of anion recognition site are simple structural component. The optical or electrochemical signals are changed upon receptor unit binding with anions. Recently, many examples of metal-based

receptors for cyanide anion such as Cu (II) complex [20-22] and Zn (II) complex [23, 24] have been reported. Special attention has been paid to Cu^{2+} complexes as sensors for cyanide (CN^-) in semi aqueous or aqueous environment utilizing the strong affinity of CN^- with Cu^{2+} [3, 4, 22, 25-27]. The copper complexes provide Cu^{2+} ions for CN^- to form very stable $[Cu(CN)_x]^{n-}$ [28]. Because the d^9 electronic configuration of Cu^{2+} displays strong binding tendencies towards CN^-, it is rationally concluded that the complexes with Cu^{2+} can detect CN^- employing high stabilization effects on the ligand field [29-36].

Extensively, metal-containing anion receptors can be conveniently classified into five categories [37] as shown in **Figure 1.5** (i) a substitutionally inert metal ion plays a structure-organising role, (ii) a generally Lewis acidic metal is a key component of the anion binding site, (iii) the metal acts as part of a redox, luminescent or colorimetric reporter group, (iv) self-assembled coordination complexes based on substitutionally labile metals involving thermodynamic anion templation, and (v) anion-binding solid-state coordination polymer networks. Certainly, there are examples of compounds that can be categorized into more than one category.

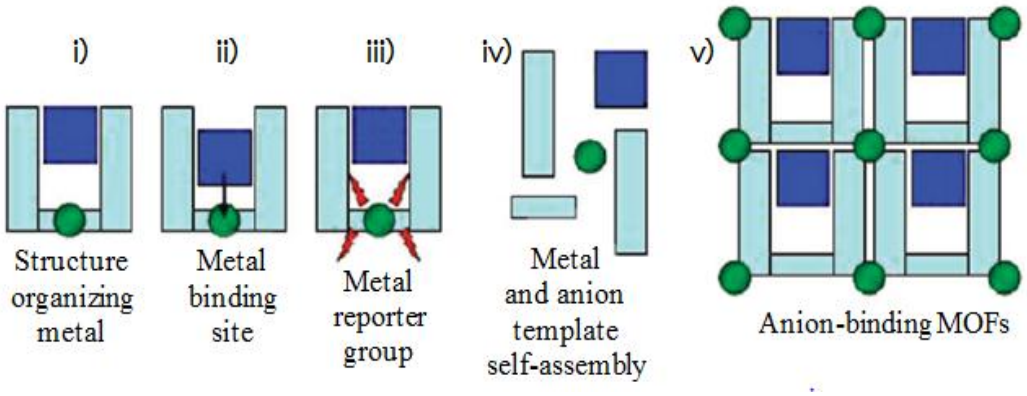

Figure 1.5 Classes of anion-binding metal complex [37].

1.2.1 Metal-based anion receptors

In 2011 Helal and co-workers [38] developed thiazole-based (**7**) to form complexes with copper. In addition, **7**-Cu^{2+} complex is used as a chemosensor for cyanide detection via the displacement approach of the copper ion as proposed in **Scheme 1.6**. In aqueous ethanol (1:1) buffered at pH 7.4, **7** displayed an obvious absorption band at 334 nm. This can be attributable to a π-π^* transition. However, upon addition of Cu^{2+} to the solution of **7**, a new absorption band at 381 nm becomes enhanced gradually, while the absorption band at 334 nm decreased synchronously, due to the disruption of hydrogen bonding between the phenolic hydrogen and thiazole nitrogen. Only the addition of CN^- to the **7**-Cu^{2+} complex solution causes a blue shift to 334 nm due to the extraction of Cu^{2+} by the CN^-. For fluorescence experiments were carried with **7**-Cu^{2+} complex results in a simultaneous quenching of fluorescent emission at 492 nm when excited at 340 nm. Upon addition of the CN^-, the peak at 492 nm, which was quenched due to the addition of Cu^{2+}, was enhanced.

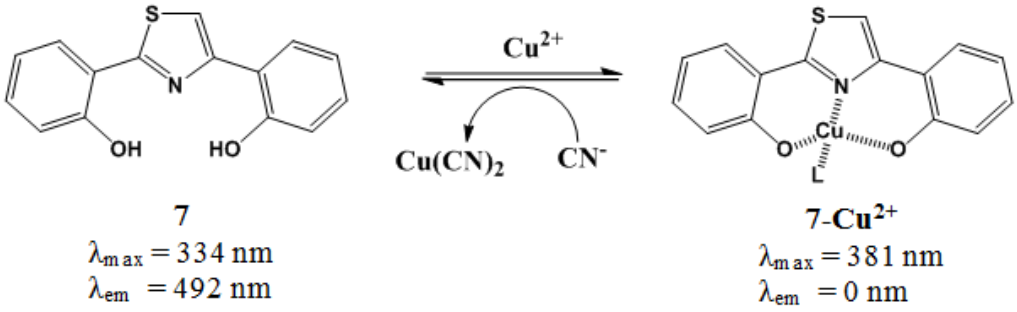

7
$\lambda_{max} = 334$ nm
$\lambda_{em} = 492$ nm

7-Cu^{2+}
$\lambda_{max} = 381$ nm
$\lambda_{em} = 0$ nm

Scheme 1.6 Proposed mechanism for cyanide sensing [38].

In 2012 Xu and co-workers [39] created benzothialzolium hemicyanine dye (**8**), including di-(2-picolyl)amine (DPA) as a Cu^{2+} receptor and an electron-donating group. Receptor **8** have a typical donor-acceptor structure with an absorption band

in the visible region is of ICT character. The cyanide recognition were achieved by the removal of Cu^{2+} in the presence of CN^- as shown in **Scheme 1.7**. Receptor **8** exhibited a fluorescence quenching effect with Cu^{2+} and the following addition of cyanide induced fluorescence enhancement in combination with a visible colorimetric change from light yellow to orange. The novel sensor shows good sensitivity with low detection limit, and displays high selectivity to cyanide more than other common anions.

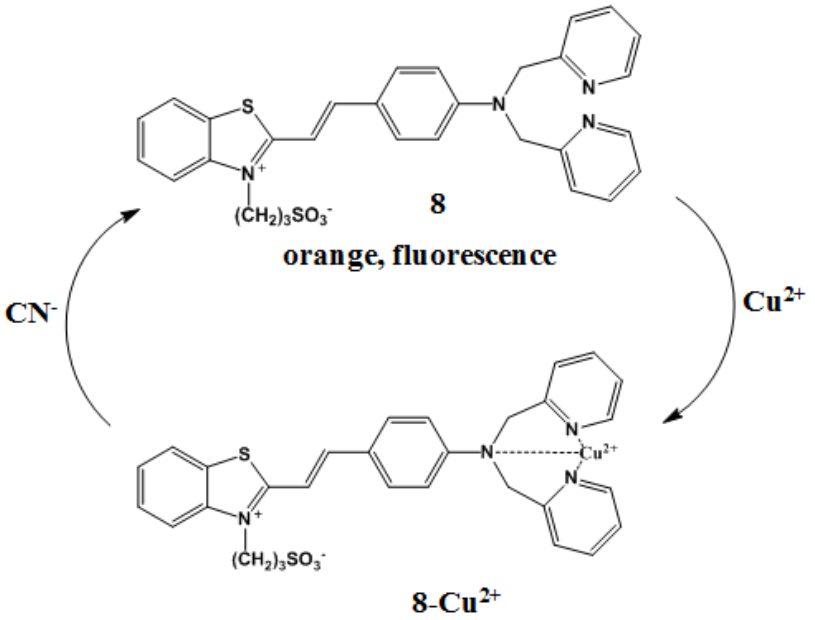

Scheme 1.7 The conversion of **8** in the presence of Cu^{2+} and CN^- [39].

In 2014 Park and co-workers [22] designed and synthesized a novel colorimetric sensor **9** for the detection of Cu^{2+}. In methanol solution, **9** showed selectivity toward Cu^{2+} in a 1:1 stoichiometry, which induces an obvious color change from yellow to purple. A bathochromic shift response was explained by the change of internal charge transfer (ICT) band. Furthermore, the chemosensing ensemble **9**-Cu^{2+} was used as a fluorescent sensor for cyanide ion. The cyanide-sensing mechanism by **9**-Cu^{2+} complex showed the two-step process, “complexation

approach" and "displacement approach" as proposed in **Scheme 1.8**. Consequently, these results may lead to the development of a new type of sequential recognition of Cu^{2+} and CN^- using two different sensing methods, color change, and fluorescence.

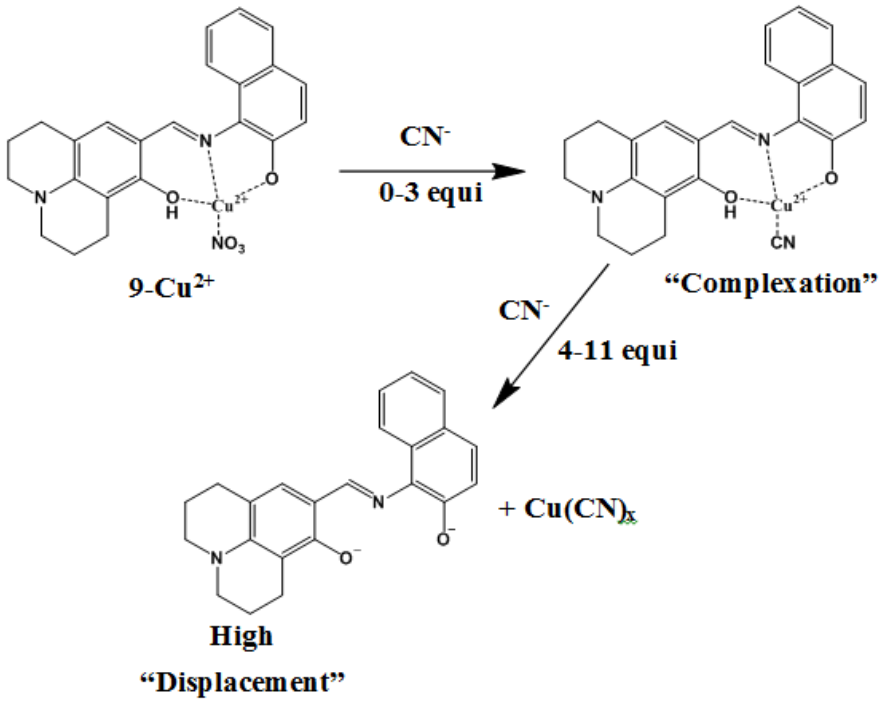

Scheme 1.8 Proposed cyanide-sensing mechanism of **9**-Cu^{2+} complex [22].

In 2014, Jo and co-workers [26] reported a new colorimetric sensor **10** based on the combination of coumarin and naphthol groups. The receptor **10** displayed highly selective and sensitive colorimetric recognition toward Cu^{2+} by color change from yellow to orange, and enabled analysis of Cu^{2+} ions with a sensitivity limit of 29.5 μM, which is below the World Health Organization (WHO) acceptable limit (31.5 μM) in drinking water. Moreover, the binding of the receptor **10** and Cu^{2+} was also chemically reversible with ethylenediaminetetraacetic acid (EDTA). Furthermore, the **10**-Cu^{2+} complex can be used as a colorimetric sensor for cyanide ion with changing its color from orange to yellow in aqueous solution. Therefore, these results may

provide to the development of a novel type of chemosensors for the sequential recognition of Cu^{2+} and CN^- by a colorimetric method in aqueous solution.

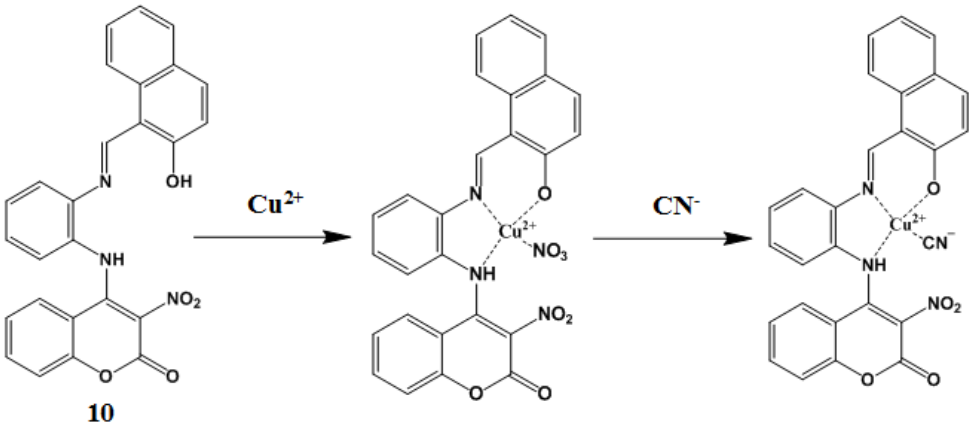

Scheme 1.9 Proposed binding mode of **10**-Cu^{2+} and **10**-Cu^{2+}-CN^- complexes [26].

In 2013 Walaijai and co-workers [40] designed and synthesized ferrocene derivative containing 2 different binding sites, including the DPA moiety for cation binding and amide group for anion binding (**Figure 1.6**). This molecule (**11**) can form complex with Cu^{2+} leading to fluorescence quenching. In the presence of CN^-, the emission spectra of **11**-Cu^{2+} shows higher emission enhancement than other anions as shown in **Figure 1.7**. Moreover, this complex can also recognize CN^- using cyclic voltammetry. Upon increasing CN^- concentration to the Cu^{2+}-complex solution gave a cathodic shift of Cu^{2+}/Cu^+ reduction wave and a irreversible of Fc/Fc^+ couple as shown in **Figure 1.8**. Therefore, the Cu^{2+}-complex is a potential optical and electrochemical sensor for cyanide anion.

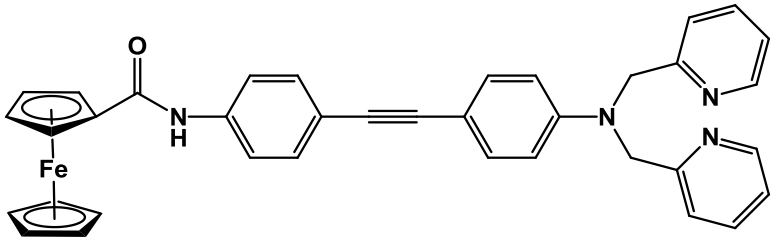

Figure 1.6 Structure of ferrocene derivative (**11**) [40].

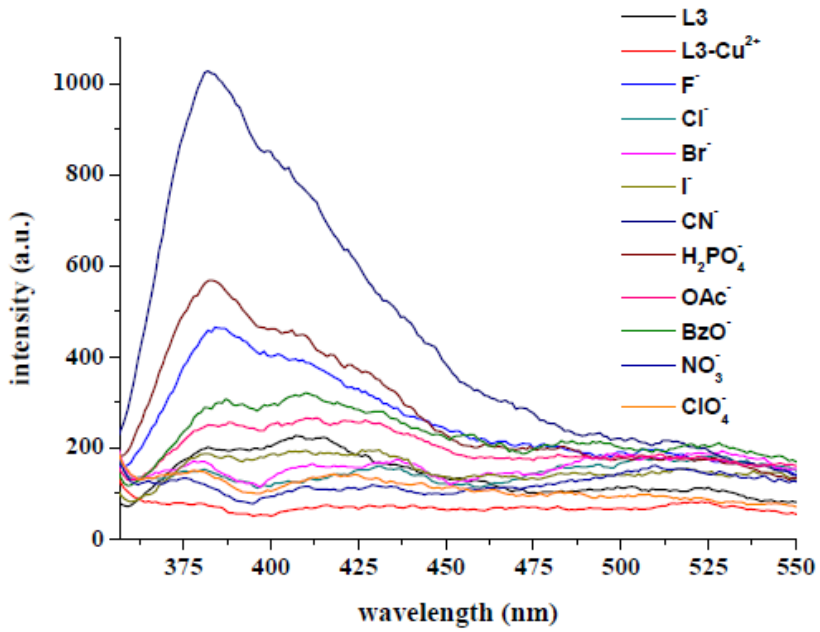

Figure 1.7 Emission spectra of **11** ($2x10^{-5}$ M in 20% CH_3CN/CH_2Cl_2) upon sequential addition of $Cu(ClO_4)_2$ (1.0 equiv.) and 40.0 equiv. of different anions as tetrabutylammonium salts [40].

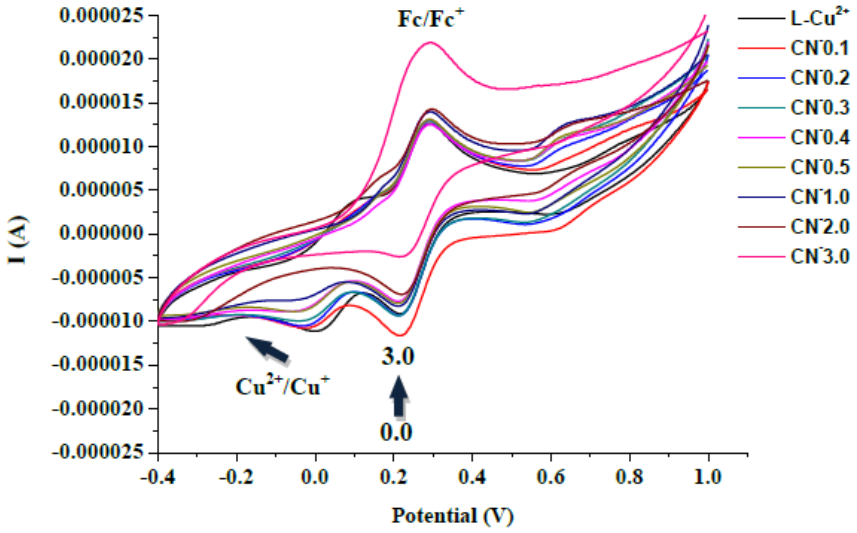

Figure 1.8 Cyclic voltammetric titration of **11** (1mM) upon sequential addition of $Cu(ClO_4)_2$ (1.0 equiv.) and titration with TBACN (0.0-3.0 equiv.) in 50% CH_3CN/CH_2Cl_2 with 0.1 M $TBAPF_6$ at a scan rate of 50 mV/s in the region of 1.0 V to -0.4 V [40].

The most of mechanism of Cu^{2+} complex for cyanide ion detection, including cyanide can coordinate at the Cu^{2+} of complex and cyanide can extract Cu^{2+} from complex.

1.3 Concept of this study

The design and synthesis of receptors that have the ability to selectivity and sensitivity to cyanide ion via electrochemical and optical response are the subject of this research. The conventional approaches for the binding of the cyanide ion have used the specific Lewis acid-base interaction [9, 11, 41-44] such as the strong affinity of a boron atom toward the cyanide ion. Therefore, in this research we have designed molecular sensor for cyanide recognition by using boronic acid as receptor unit. In addition, the designed metal-based receptors are widely used for cyanide detection. Therefore, we have designed the 2,2, dipicolylamine (DPA) unit for a metal ion receptor in coordination chemistry and complex can act as anion monitoring. The combination of ferrocene redox-active unit with receptor unit through the **π**-conjugated aryl ethyne spacer is expected to result in changer optical and/or electrochemical signals.

1.4 Objective and scope of the research

1. To synthesize and characterize unsymmetrically ferrocene derivative incorporating boronic acid and dipicolylamine (DPA) receptors (**L1** and **L2**), respectively.
2. To study the sensing abilities of molecular sensor (**L1 and L2**) by using UV-Vis spectrophotometry and cyclic voltammetry.

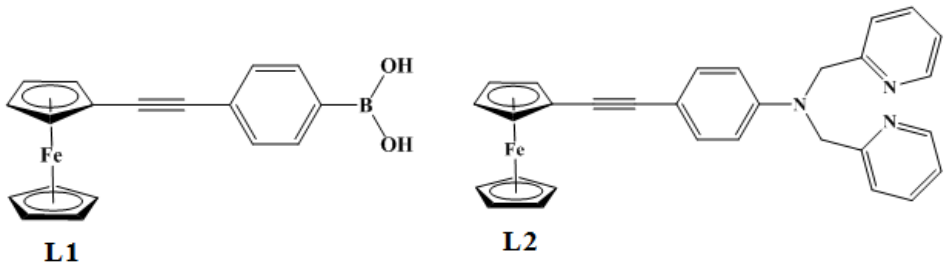

Figure 1.9 Structures of molecular sensors **L1** and **L2**.

CHAPTER II

EXPERIMENTAL

2.1 General Procedure

2.1.1 Materials

All chemicals and solvents were of analytical grade obtained from Fluka, Aldrich, Carlo Erba, Merck or Lab Scan and used without further purification. Tetrahydrofuran (THF) was distilled over sodium and benzophenone. Toluene was dried over calcium hydride under nitrogen and distilled prior to use. Column chromatography was carried out using silica gel (Kieselgel 60, 0.063 – 0.200 mm, Merck) and aluminium oxide 90 standardized (0.063 – 0.200 mm, Merck). Thin layer chromatography (TLC) was performed on silica gel plates (Kieselgel 60, F_{254}, Merck) and aluminium oxide plates (aluminium oxide 60, F_{254}, neutral, Merck).

2.1.2 Analytical measurements

Nuclear Magnetic Resonance (NMR) spectra were recorded on a Varian Mercury plus 400 NMR or a Bruker Avance 400 NMR spectrometer. All chemical shifts were reported in part per million (ppm) using the residual proton or carbon signals in deuterated solvents. MALDI–TOF mass spectra were recorded on a Biflex Mass Spectrometer using 2–cyano–4–hydroxycinnamic acid (CCA) as a matrix. The purity of the desired product was checked by elemental analysis using a CHNS/O analyzer (Perkin Elmer PE2400 series II). All UV–Vis spectra were recorded with a Varian Cary 50 UV–Vis spectrophotometer. All fluorescence spectra were measured by a Varian Cary Eclipse fluorescence spectrophotometer. Cyclic voltammetry (CV) was performed using a μ–AUTOLAB TYPE III potentiostat. All electrochemical experiments were carried out with three electrode cells comprising of a working electrode,

a counter electrode and a reference electrode operating at room temperature. A platinum electrode with a diameter 3 mm was used as a working electrode. A Pt wire was used as a counter electrode. A silver wire immersed in 0.01 M silver nitrate solution was used as a reference electrode.

2.2 Synthesis

2.2.1 Synthesis of L1

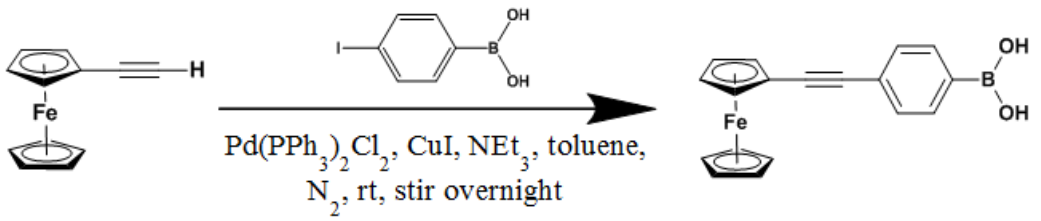

4–Iodophenyl boronic acid (0.124 g, 0.5 mmol), $Pd(PPh_3)_2Cl_2$ (0.012 g, 0.02) and CuI (0.006 g, 0.03 mmol) were placed in a 50 mL two–necked round bottom flask equipped with a magnetic bar. The reaction was purged with nitrogen gas in a balloon. A mixed solvent (10 mL, NEt_3/toluene 1:1 v/v) was added to the reaction vessel. The mixture was stirred for 30 minutes at room temperature and then ethynylferrocene (0.105 g, 0.5 mmol) was added to the reaction vessel. After stirring under nitrogen for overnight at room temperature, solvent was removed under vacuum and the solid was filtered and washed with water (30 mL) and CH_2Cl_2 (3x30 mL). The organic layer was dried over anhydrous Na_2SO_4, filtered and the solvent was removed under reduced pressure. The crude product was purified by column chromatography on SiO_2 using mixed solvents (10%–60% EtOAc/hexane) as eluent to afford **L1** as an orange solid (0.074 g, 45% yield).

Characterization data for L1

^{1}H NMR: δ_H (400 MHz, CD_3OD, ppm) 4.25 (s, Fc–H_c, 5H), 4.30 (s, Fc–H_b, 2H), 4.51 (s, Fc–H_a, 2H), 7.42 (t, J = 8.0 Hz, Ar–H_d, 2H), 7.61 (d, J = 8.0 Hz, Ar–H_e, 1H), 7.74 (d, J = 8.0 Hz, Ar–H_f, 1H).

^{13}C NMR: δ_C (100 MHz, CD_3OD, ppm) 66.22, 69.68, 70.71, 72.44, 86.46, 86.61, 90.05, 126.79, 131.02, 134.36, 134.62.

MS (MALDI–TOF) calcd. for $[M]^+$ *m/z* 330.1, found 329.2 $[M]^+$.

Elemental analysis calcd. for $C_{18}H_{15}BFeO_2$: C, 65.52%; H, 4.58%, found: C, 65.49%; H, 4.54%.

2.2.2 Synthesis of 4–iodo–*N*,*N*–bis(pyridin–2–ylmethyl)aniline (2a)

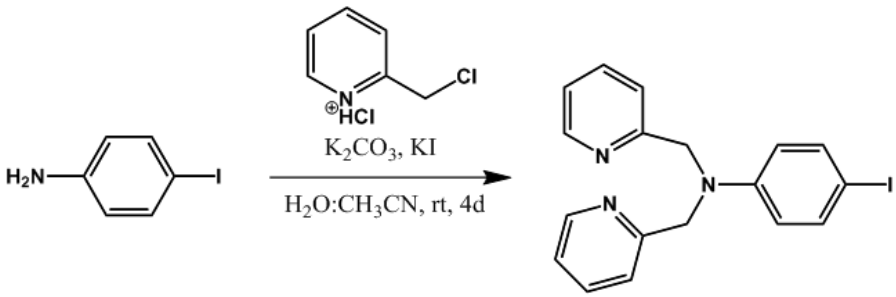

K_2CO_3 (2.2 g, 16.00 mmol) was slowly added to a stirred solution of 2–picolyl chloride hydrochloride (1.3 g, 8.00 mmol) and potassium iodide (0.7 g, 4.80 mmol) in water (3 mL). Then, a solution of 4–iodoaniline (0.7 g, 3.20 mmol) in acetonitrile (2 mL) was added to the stirred mixture. The reaction mixture was stirred vigorously for 4 days at room temperature. It was diluted with CH_2Cl_2 30 mL, filtered and washed

with water (30 mL). The aqueous layer was extracted with CH_2Cl_2 (3x20 mL). The organic layer was dried over anhydrous Na_2SO_4, filtered, and the solvent was removed under reduced pressure. The crude product was purified by column chromatography (SiO_2) using 10%–60% EtOAc/CH_2Cl_2 as eluent and recrystallized from CH_2Cl_2/hexane to yield **2a** as a white crystal (0.398 g, 31% yield).

Characterization data for 2a

^{1}H NMR: δ_H (400 MHz, $CDCl_3$, ppm) 4.79 (s, C*H*$_2$, 4H), 6.47 (d, *J* = 8.0 Hz, Ar–*H*, 2H), 7.16–7.26 (m, Py–*H*, 4H), 7.38 (d, *J* = 8.0 Hz, Ar–*H*, 2H), 7.62 (t, *J* = 8.0 Hz, Py–*H,* 2H) 8.58 (d, *J* = 4.0 Hz, Py–*H*, 2H).

^{13}C NMR: δ_C (100 MHz, $CDCl_3$, ppm) 57.3, 78.3, 114.9, 120.7, 122.2, 136.8, 137.8, 147.8, 149.7, 158.2.

MS (MALDI–TOF) calcd. for $[M]^+$ *m/z* 401.0, found 399.3 $[M]^+$.

2.2.3 Synthesis of L2

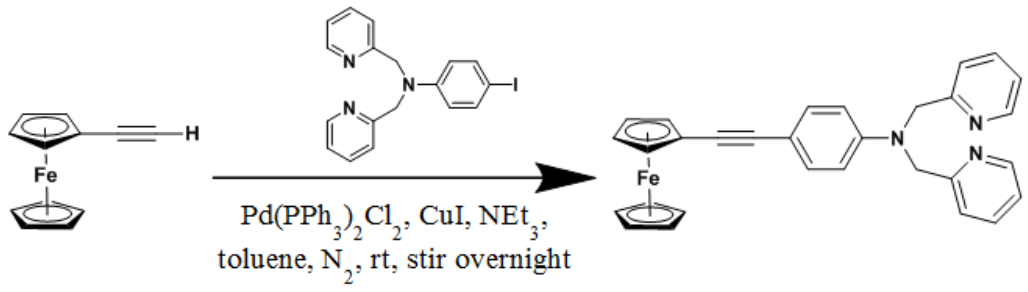

Compound **2a** (0.320 g, 0.80 mmol), $Pd(PPh_3)_2Cl_2$ (0.012 g, 0.02 mmol) and CuI (0.006 g, 0.03 mmol) were placed in a 50 mL two–neck round bottom flask equipped with a magnetic bar. The reaction was purged with nitrogen in a balloon. A mixed

solvent (12 mL, NEt_3/toluene 1:1 v/v) was added to the reaction vessel. The mixture was stirred for 30 minutes at room temperature and then ethynylferrocene (0.105 g, 0.50 mmol) was added to the reaction vessel. After stirring under nitrogen for overnight at room temperature, the reaction mixture was filtered, eluted with CH_2Cl_2 and the filtrate was evaporated. The crude product was purified by column chromatography (SiO_2) using gradient mixed solvents (0%–50% EtOAc/CH_2Cl_2) as eluent and recrystallized in CH_2Cl_2/hexane to afford **L2** as an orange solid (0.161 g, 67% yield).

Characterization data for L2

^{1}H NMR: δ_H (400 MHz, $CDCl_3$, ppm) 4.18 (s, Fc–*H*, 5H), 4.20 (s, Fc–*H*, 2H), 4.43 (s, Fc–*H*, 2H), 4.84 (s, C*H*$_2$, 4H), 6.64 (d, *J* = 8.0 Hz, Ar–*H*, 2H), 7.27 (dd, J_{AB} = 7.6 Hz, J_{AC} = 1.6 Hz, Py–*H*, 2H), 7.23 (d, *J* = 7.6 Hz, Py–*H*, 2H), 7.28 (d, *J* = 8.8 Hz, Ar–*H*, 2H), 7.63 (t, *J* = 8.0 Hz, Py–*H*, 2H), 8.60 (d, *J* = 4.0 Hz, Py–*H*, 2H).

^{13}C NMR: δ_C (100 MHz, $CDCl_3$, ppm) 57.3, 68.4, 68.5, 69.9, 71.2, 85.8, 86.1, 112.4, 120.8, 122.1, 132.7, 136.8, 147.5, 147.7, 149.8, 158.4.

MS (MALDI–TOF) calcd. for $[M]^+$ *m/z* 483.1, found 482.6 $[M]^+$.

Elemental analysis calcd. for $C_{30}H_{25}FeN_3$: C, 74.54%; H, 5.21%; N, 8.69%, found: C, 74.57%; H, 5.21%; N, 8.65%.

2.3 Electrochemical studies of L1

2.3.1 Chemicals

All chemicals and solvents were standard analytical grade. Anions selected in this study are acetate (AcO^-), perchlorate (ClO_4^-) as tetrabutylammonium salts, benzoate (BzO^-) as tetraethylammonium salts, chloride (Cl^-) as sodium salts, fluoride (F^-), chloride (Cl^-), bromide (Br^-), iodide (I^-) and cyanide (CN^-) as potassium salts. Tetrabutylammonium hexafluorophosphate ($TBAPF_6$) was used to prepare a supporting electrolyte solution. Silver nitrate ($AgNO_3$) was used as the inner reference solution in reference electrode.

2.3.2 Experimental procedure

The supporting electrolyte is 0.1 M tetrabutylammonium hexafluorophosphate ($TBAPF_6$) in CH_3CN. The surface of working electrode was polished with 1.0 μm followed by 0.3 μm of slurry alumina powder, and then rinsed with water. The residue of alumina particles were thoroughly eliminated by sonicating for 5 minutes in 0.05 M H_2SO_4. The electrode was rinsed again with water followed by acetone, and dried. The $Ag/AgNO_3$ electrode, composing of a silver wire immersed in a solution of 0.01 M $AgNO_3$ in 0.1 M $TBAPF_6$, was used as a reference electrode. The solution was purged with nitrogen for 3 minutes to eliminate oxygen before performing the experiment at room temperature. The scan rate for this study is 100 mV/s.

2.3.3 Electrochemical studies of L1 with various anions

Generally, a 0.001 M solution of a receptor **L1** in 5 mL of 0.1 M $TBAPF_6$ in CH_3CN as supporting electrolyte was prepared. A 0.1 M solution of anions was also prepared in the supporting electrolyte solution. The solution of each anions

(1 equiv.) was added into the solution of the receptor and stirred for 3 minutes prior to measure.

2.3.4 Electrochemical titration of L1 with fluoride compared with cyanide anion

Ligand **L1** (0.001 M) in 5 mL of 0.1 M of supporting electrolyte was prepared. The solution of cyanide anion (0.1 M, in supporting electrolyte solution) was prepared in 1 mL of a vial. Each anion solution was added in a portion to the solution of the receptor and stirred for 3 minutes prior to measure. Amounts of added fluoride and cyanide were listed in **Table 2.1** and **Table 2.2**, respectively.

Table 2.1 Volume and concentration of fluoride ion solution used in the CV titration of **L1**

Equivalents of fluoride ion	Added volume of 0.1 M of fluoride ion solution (μL)	Concentration of fluoride ion (M)	Concentration of receptor **L1** (M)
0	0	0	1.00×10^{-3}
1	50	9.90×10^{-4}	9.90×10^{-4}
5	250	4.76×10^{-3}	9.52×10^{-4}
10	500	9.09×10^{-3}	9.09×10^{-4}

Table 2.2 Volume and concentration of cyanide ion solution used in the CV titration of **L1**

Equivalents of cyanide ion	Added volume of 0.1 M of cyanide ion solution (μL)	Concentration of cyanide ion (M)	Concentration of receptor **L1** (M)
0	0	0	1.00×10^{-3}
0.5	25	4.98×10^{-4}	9.95×10^{-4}
1.0	50	9.90×10^{-4}	9.90×10^{-4}
1.5	75	1.48×10^{-3}	9.85×10^{-4}
2.0	100	1.96×10^{-3}	9.80×10^{-4}
2.5	125	2.44×10^{-3}	9.76×10^{-4}
3.5	175	3.38×10^{-3}	9.66×10^{-4}
5.0	250	4.76×10^{-3}	9.52×10^{-4}

2.4 ^{1}H NMR spectral studies of L1

2.4.1 Chemicals

All materials were standard analytical grade. The solvent is MeOH–d_4 (D, 99.8%). Anions selected in this study is potassium cyanide.

2.4.2 ^{1}H NMR titration of L1 with cyanide anion

Ligand **L1** (0.0746 M) in 0.4 mL of MeOH–d_4 was prepared in NMR tube. The solution of cyanide anion (0.1 M, in MeOH–d_4) was prepared in 1 mL of a vial. The cyanide solution was added in a portion to the solution of the receptor. Amounts of added cyanide were listed in **Table 2.3**.

Table 2.3 Volume and concentration of cyanide ion solution used in the ^{1}H NMR titration of **L1**

Equivalents of cyanide ion	Added volume of 0.61 M of cyanide ion solution (μL)	Concentration of cyanide ion (M)	Concentration of receptor **L1** (M)
0	0	0	7.46×10^{-2}
0.5	24	3.45×10^{-2}	7.04×10^{-2}
1.0	48	6.54×10^{-2}	6.66×10^{-2}
2.0	96	1.18×10^{-1}	6.02×10^{-2}
5.0	240	2.29×10^{-1}	4.66×10^{-2}

2.5 UV–Vis spectrophotometry studies of L2

2.5.1 Chemical

All materials were standard analytical grade. The solvents were spectrochemical grade. Cations selected in this study are manganese (II), cobalt (II), nickel (II), zinc (II), copper (II) perchlorate. Anions selected in this study are fluoride (F^-), chloride (Cl^-), bromide (Br^-), iodide (I^-), hydroxide (OH^-), perchlorate (ClO_4^-), dihydrogen phosphate ($H_2PO_4^-$), acetate (AcO^-), nitrate (NO_3^-) as tetrabutylammonium salts, benzoate (BzO^-), cyanide (CN^-) as tetraethylammonium salts.

2.5.2 UV–Vis spectrophotometry studies of L2 with various cations

The solution of ligand **L2** ($2.5\text{x}10^{-5}$ M) in CH_3CN. A portion (2 mL) of this solution was pipetted into a 1 cm pathlength quartz cuvette. All solutions of each cations ($1\text{x}10^{-2}$M) were prepared in of a vial (2 mL). Each cation solution (25 μL, 5.0 equiv.) was transferred to the cuvette and stirred for 5 minutes before measurement.

2.5.3 UV–Vis spectrophotometry titration of L2 with copper (II) ion

The solution of ligand **L2** ($2.5x10^{-5}$ M) in CH_3CN. A portion (2 mL) of this solution was pipetted into a 1 cm pathlength quartz cuvette. A 0.01 M solution of copper (II) ion was also prepared in of a vial (2 mL). The solution of copper (II) ion was added into the solution of the **L2** and stirred for 5 minutes before each scan. Amounts of added copper (II) ion were listed in **Table 2.4**.

Table 2.4 Volume and concentration of copper (II) ion solution used in the UV–Visible titration of **L2**

Equivalents of copper(II) ion	Added volume of 0.01 M of copper (II) ion solution (μL)	Concentration of copper(II) ion (M)	Concentration of receptor **L2** (M)
0	0	0	2.50×10^{-5}
1	5	2.49×10^{-5}	2.49×10^{-5}
3	15	7.44×10^{-5}	2.48×10^{-5}
5	25	1.23×10^{-4}	2.47×10^{-5}

2.5.4 UV–Vis spectrophotometry studies of L2-Cu^{2+} with various anions

A mixture of receptor **L2** ($2x10^{-5}$ M) in CH_3CN and 1.0 equiv. of Cu^{2+} ion was prepared. The 2 mL of ligand **L2** solution was transfered to a 1 cm pathlength quartz cuvette. Then, the 5 μL of Cu^{2+} solution (1.0 equiv.) was added to the cuvette and stirred for 5 minutes before adding each anion. The solution of anionic guest (0.01 M, CH_3CN was prepared in a vial (1 mL). The 15 μL (3.0 equiv.) of each anionic guest solution was transferred to the cuvette and stirred for 5 minutes before each scan.

2.6 Electrochemical studies of L2

2.6.1 Chemicals

All chemicals and solvents were standard analytical grade. Cations selected in this study are manganese (II), cobalt (II), nickel (II), zinc (II), copper (II) perchlorate. Anions selected in this study are fluoride (F^-), dihydrogen phosphate ($H_2PO_4^-$) as tetrabutylammonium salts, cyanide (CN^-) as tetraethylammonium salts.

2.6.2 Experimental procedure

The supporting electrolyte is 0.1 M $TBAPF_6$ in CH_3CN. The surface of working electrode was polished with 1.0 μm followed by 0.3 μm of slurry alumina powder, and then rinsed with water. The residue of alumina particles were thoroughly eliminated by sonicating for 5 minutes in 0.05 M H_2SO_4. The electrode was rinsed again with water followed by acetone, and dried. The $Ag/AgNO_3$ electrode, composing of a silver wire immersed in a solution of 0.01 M $AgNO_3$ in 0.1 M $TBAPF_6$, was used as a reference electrode. The solution was purged with nitrogen gas for 3 minutes to eliminate oxygen before performing the experiment at room temperature. The scan rate for this study is 50 mV/s.

2.6.3 Electrochemical studies of L2 with various cations

Generally, 1 mM solution of **L2** in 5 mL of supporting electrolyte was prepared. All solutions of each cations (0.1 M) were prepared in the supporting electrolyte solution in of a vial (2 mL). The solution of each cations (50 μL, 1.0 equiv.) was added into the solution of **L2** before measurement.

2.6.4 Electrochemical titration of L2 with copper (II) ion

Ligand **L2** (0.001 M) in 5 mL of 0.1 M of supporting electrolyte was prepared. The solution of copper (II) ion (0.1 M, in supporting electrolyte solution) was prepared in 1 mL of a vial. Copper (II) ion solution was added in a portion to the solution of the receptor and stirred for 3 minutes prior to measure. Amounts of added fluoride and cyanide copper (II) ion were listed in **Table 2.5**.

Table 2.5 Volume and concentration of cyanide ion solution used in the CV titration of **L2**

Equivalents of copper(II) ion	Added volume of 0.1 M of copper (II) ion solution (μL)	Concentration of Copper (II) ion (M)	Concentration of receptor **L2** (M)
0	0	0	1.00×10^{-3}
0.1	5	9.99×10^{-5}	9.99×10^{-4}
0.3	15	2.99×10^{-4}	9.97×10^{-4}
0.5	25	4.98×10^{-4}	9.95×10^{-4}
1.0	50	9.90×10^{-4}	9.90×10^{-4}
1.5	75	1.48×10^{-3}	9.85×10^{-4}

2.6.5 Electrochemical studies of L2-Cu^{2+} with various anions

A mixture of ligand **L2** (1 mM) in 5 mL of 0.1 M of $TBAPF_6$ in CH_3CN as supporting electrolyte and 1.0 equiv. of copper (II) ion (copper (II) perchlorate hexahydrate, $Cu(ClO_4)_2{\cdot}6H_2O$) was prepared. The 50 μL (1.0 equiv.) of 0.1 M copper (II) solution was added to the solution of the receptor, and then stirred for 5 minutes before the addition of the anion. The solution of each anion (0.1 M, in supporting electrolyte solution) was prepared in 1 mL of a vial. Each anion solution

(50 μL, 1.0 equiv.) was added in a portion to the solution of the receptor and stirred for 5 minutes prior to measure.

2.7 Computational studies of L2-Cu^{2+} complex in the presence of CN^- and F^- anions

All structure-optimizations were performed with the DFT (B3LYP) method with the LANL2DZ basis sets, using the GAUSSIAN 09 program [45]. Initial structures for all studied species were prepared and visualized using the GaussView 5.0.9 program [46].

CHAPTER III

RESULTS AND DISCUSSION

3.1 Synthesis and characterization of receptor L1

The synthetic pathway of **L1** is shown in **Scheme 3.1**. **L1** has been synthesized using the Sonogashira coupling in a one–pot reaction. 4–Iodophenyl boronic acid reacted with ethynylferrocene under Sonogashira condition using $PdCl_2(PPh_3)_2$, CuI and NEt_3 as base to form orange solid product in moderate yield (45%).

The structure of desired product **L1** was characterized by ^{1}H NMR, ^{13}C NMR, COSY, HSQC, HMBC, mass spectroscopy and elemental analysis. The ^{1}H NMR spectrum of **L1** displayed well–resolved peaks appeared as a singlet peak at 4.01, 4.05 and 4.27 ppm, which were the characteristic of ferrocene unit. The signal of aromatic group was observed in the region of 7.16–7.49 ppm. In ^{13}C NMR spectrum, the signals at 86.61 and 90.05 ppm corresponded to the unsymmetrical carbon-carbon triple bond. The MALDI–TOF mass spectrum confirmed the structure of **L1** by showing an intense peak at 329.2 *m/z* $[\mathbf{L1}]^{+}$. In addition, elemental analysis also confirmed the proposed structure and the purity of this compound. The assignment of protons and carbons in this compound was determined by COSY, HSQC and HMBC experiments.

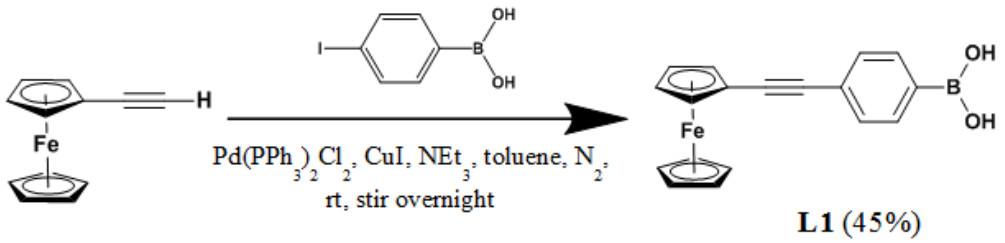

Scheme 3.1 Synthetic pathway of **L1**.

The HSQC (Heteronuclear Single Quantum Coherence) spectrum (**Figure 3.1**) shows a proton that is attacked to a carbon atom. From this spectrum, each proton can be distinguished and assigned clearly. In addition, the HMBC (Heteronuclear Multiple Bond Correlation) spectrum (**Figure 3.2**) displays a correlation of proton and carbon atoms over longer ranges of 2-4 bonds. The results of this spectrum can be used to confirm the position of H_a, H_d, H_e and H_f protons.

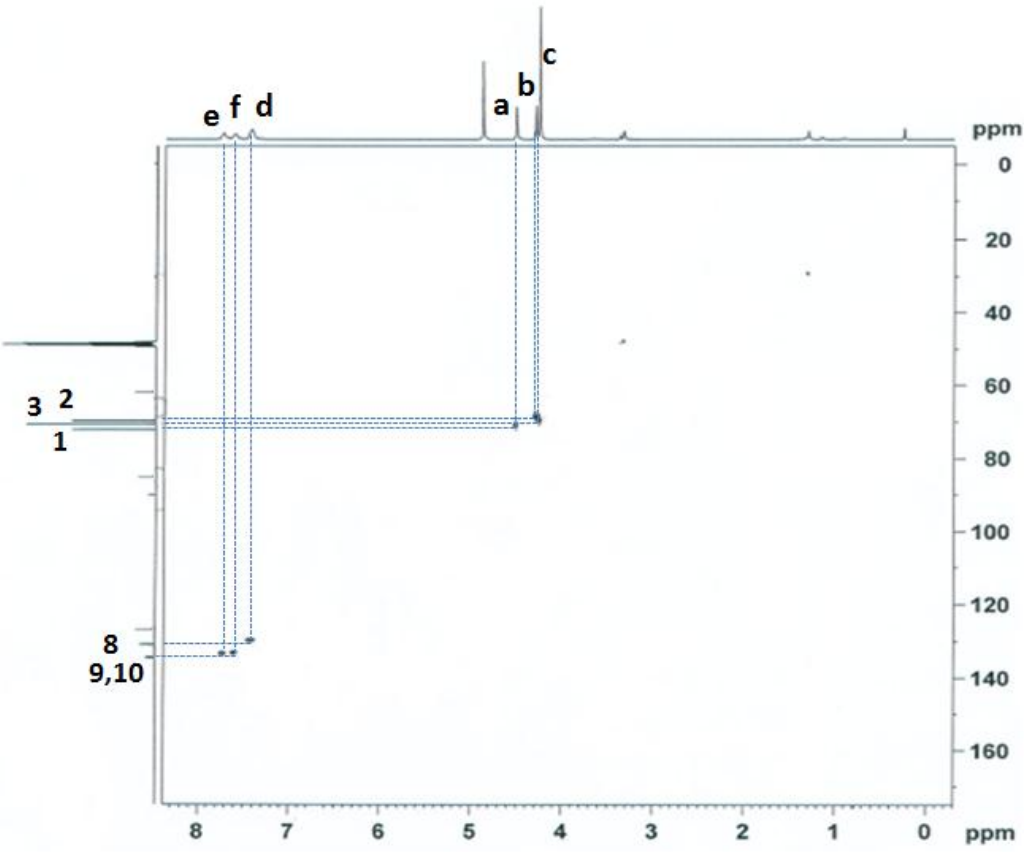

Figure 3.1 HSQC spectrum of **L1** in CD_3OD.

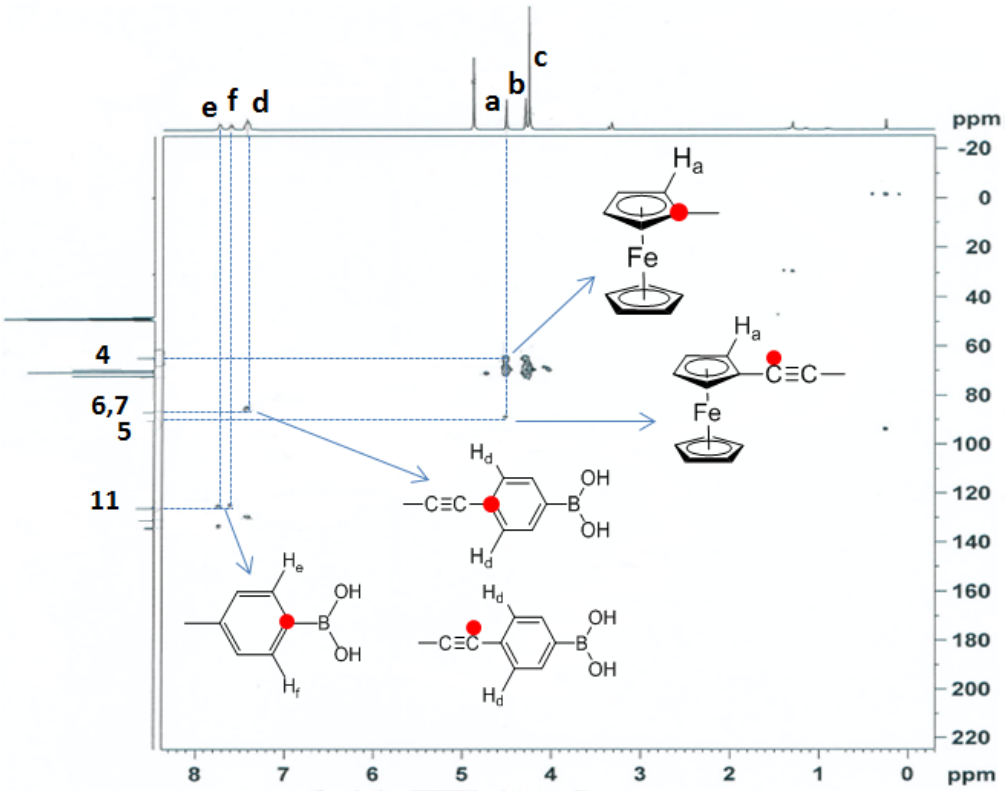

Figure 3.2 HMBC spectrum of **L1** in CD_3OD.

From the HSQC and HMBC spectra, each proton and carbon atoms of **L1** can be assigned as shown in **Figure 3.3**.

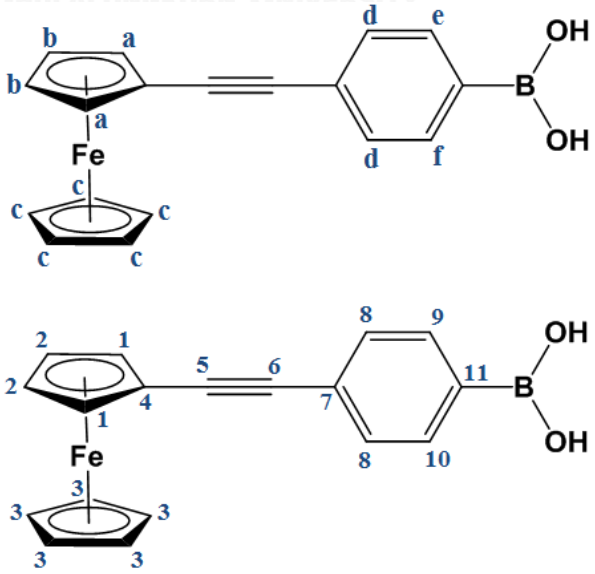

Figure 3.3 Assignment of proton (top) and carbon (bottom) of **L1**.

3.2 Synthesis and characterization of receptor L2

Synthetic pathway of compound **L2** is shown in **Scheme 3.2**. **L2** was successfully synthesized via two step. The nucleophilic substitution of picolyl chloride by 4–iodoaniline was carried out by using K_2CO_3 as base and KI as phase transfer catalyst in 1:3 H_2O/CH_3CN. The reaction completed after stirring at room temperature for 4 days and the crude product was purified to give compound **2a** as a white crystal in 31% yield. Compound **2a** was then used for coupling with ethynylferrocene to generate compound **L2** via Sonogashira coupling. This reaction was carried out following the previous literature [47] with modifications using $Pd(PPh_3)Cl_2$ as the catalyst, toluene and triethylamine as solvent and base, respectively. The reaction was stirred under nitrogen at room temperature overnight to obtain product **L2** as a orange solid in 67% yield.

The structure of desired product **L2** was characterized by ^{1}H NMR, ^{13}C NMR, COSY, HSQC, HMBC, mass spectroscopy and elemental analysis. The ^{1}H NMR spectrum of **L2** displayed well-resolved characteristic peaks of 2,2'–dipyridylamine (DPA) moiety and the signals of phenyl group in the region of 6.0-9.0 ppm. The methylene protons of DPA moiety appeared at 4.84 ppm and the signals of cyclopentadiene protons in mono–substituted ferrocene appeared at 4.18, 4.20 and 4.43 ppm. In ^{13}C NMR spectrum, the signals at 85.8 and 86.1 ppm corresponded to the unsymmetrical carbon-carbon triple bond. The MALDI-TOF mass spectrum confirmed the structure of **L2** by showing an intense peak at 482.6 *m/z* $[\mathbf{L2}]^{+}$. In addition, the assignment of protons in this compound was determined by COSY, HSQC and HMBC experiments. Elemental analysis was also confirmed the structure and the purity of this compound.

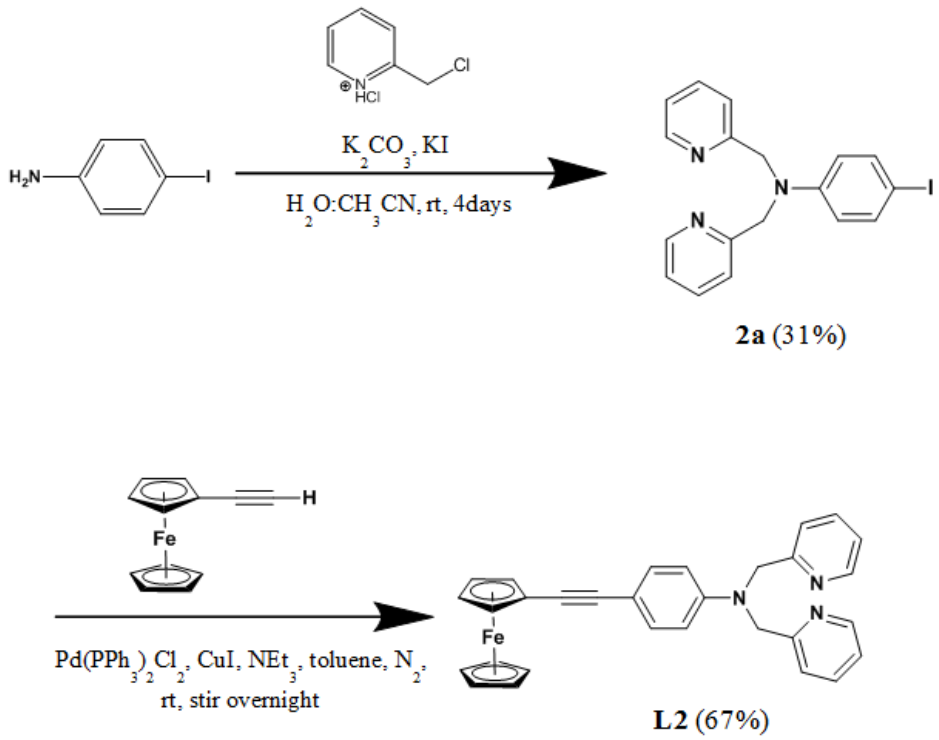

Scheme 3.2 Synthetic pathway of **L2**.

3.3 Electrochemical studies of L1

3.3.1 Electrochemical studies of L1 with various anions

The anion recognition properties of the **L1** were investigated using cyclic voltammetry (CV) in CH_3CN. **L1** showed a redox couple at $E_{1/2}$ = 0.211 V due to Fe^{2+}/Fe^{3+} of the ferrocene unit. As a representative case, the CV behaviour of the receptor **L1** in the presence of 1 equiv. of various anions (CN^-, F^-, Cl^-, NO_3^-, AcO^-, BzO^-, ClO_4^-) were shown in **Figure 3.4**. The results indicated that upon addition of the others anions (except CN^- ions) the potential of the redox couple showed no or very little variation. For fluoride ions bind very weekly with **L1** as shown in green line (**Figure 3.4b**). However, addition of CN^- ions to the solution of **L1** affects the redox property of the receptor significantly **(Figure 3.4b)**.

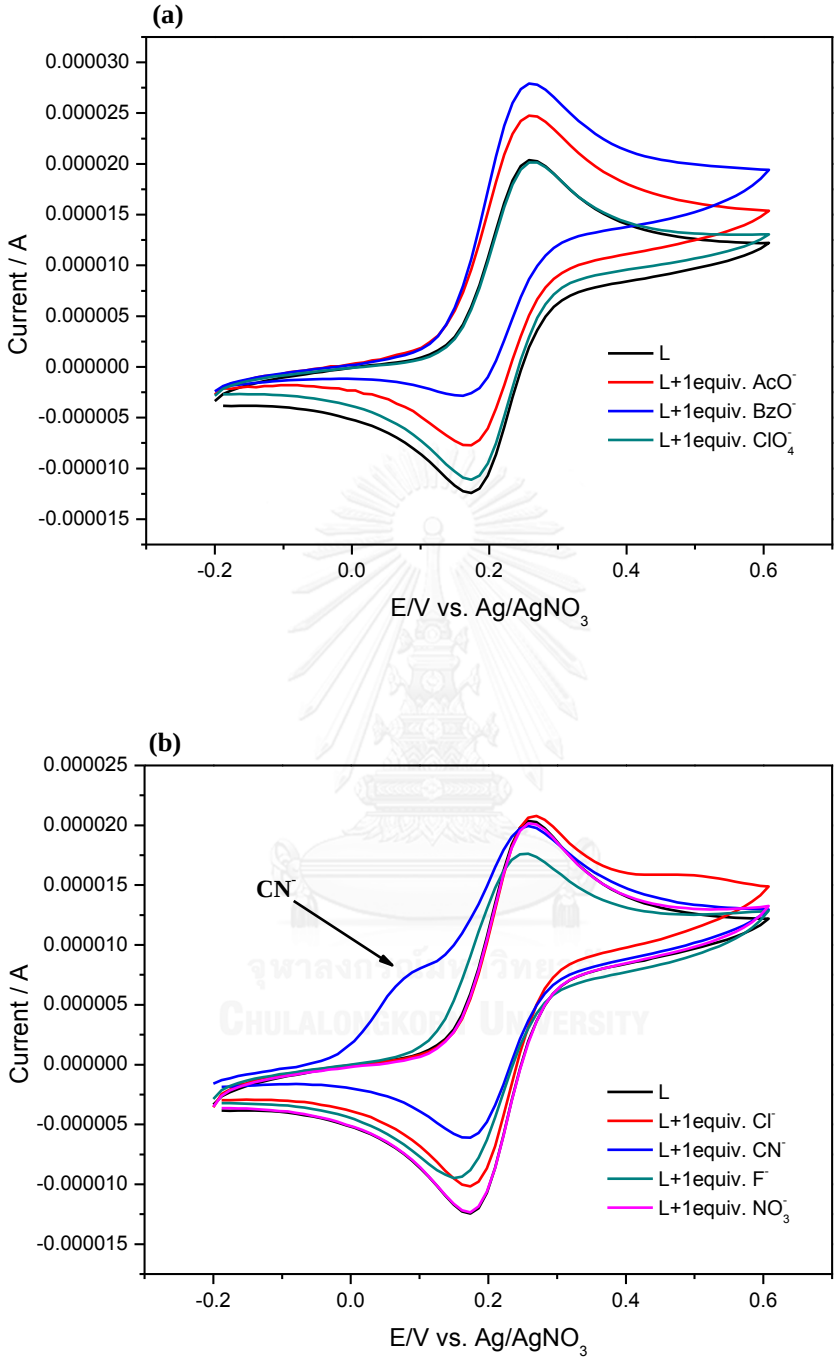

Figure 3.4 Cyclic voltammogram of **L1** (1 mM in CH_3CN with 0.1 M $TBAPF_6$) in the presence of various anions (1 equiv.) (a) AcO^-, BzO^-, $ClO4^-$ (b) CN^-, F^-, Cl^-, NO_3^- at a scan rate of 100 mV/s in the region of -0.2 V to 0.6 V.

3.3.2 Electrochemical titration of L1 with fluoride compared with cyanide anion

To understand the binding property of **L1** toward F^- and CN^- under electrochemical condition, the cyclic voltammograms of **L1** in the presence of different concentration of F^- and CN^- ions were recorded in CH_3CN solution using 0.1 M $TBAPF_6$ as the supporting electrolyte at a scan rate of 100 mV/s. Cyclic voltammograms were shown in **Figure 3.5 and Figure 3.6**. Cyclic voltammograms of the free receptor **L1** exhibited a single reversible wave at $E_{1/2}$ 0.211 V for the Fc/Fc^+ redox couple. Upon addition of F^- ions from 0–10 equiv. (**Figure 3.5**), the potential of the redox couple showed very little variation. Furthermore, the cathodic shift was observed and the new peak appeared at 0.078 V and exhibited completely irreversible of Fc/Fc^+ couple upon adding 5 equiv. of cyanide (**Figure 3.6**). This indicates the CN^- binding event occurring at the boronic acid site through the shift of the redox potential of the ferrocene moiety. Therefore, receptor **L1** has high selectivity for detecting cyanide ion.

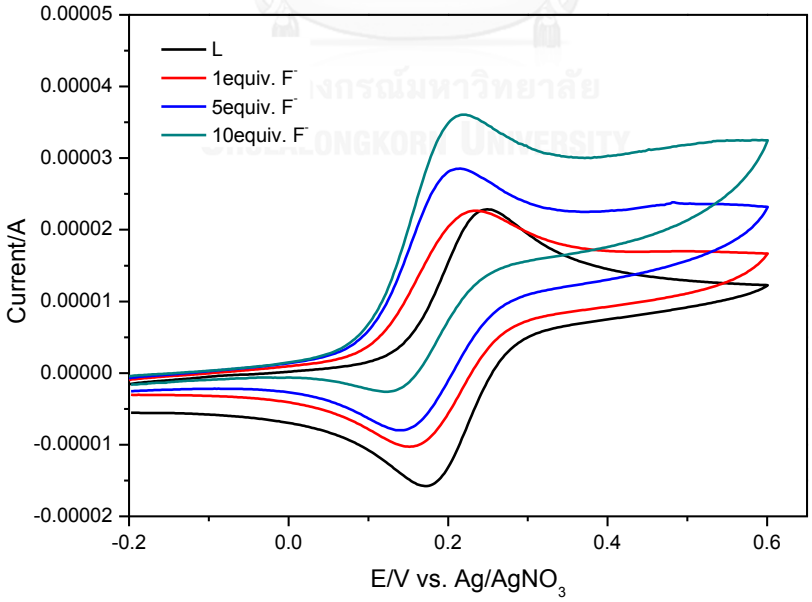

Figure 3.5 Cyclic voltammogram of **L1** (1 mM in CH_3CN with 0.1 M $TBAPF_6$) upon titration with F^- (0.0–10.0 equiv.) at a scan rate of 100 mV/s in the region of -0.2 V to 0.6 V.

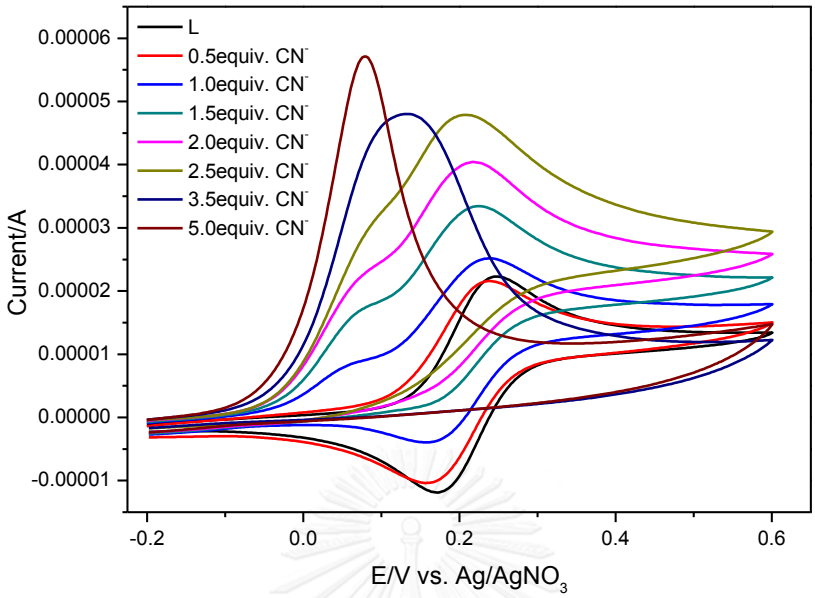

Figure 3.6 Cyclic voltammogram of **L1** (1 mM in CH_3CN with 0.1 M $TBAPF_6$) upon titration with CN^- (0.0–5.0 equiv.) at a scan rate of 100 mV/s in the region of -0.2 V to 0.6 V.

However, the voltammogram of **L1**-CN^- caused irreversible peak which suggesting that the oxidized species of **L1**-CN^- may deposit on the electrode surface.

3.4 ^{1}H NMR spectral studies

3.4.1 ^{1}H NMR titration of L1 with cyanide anion

In order to study the complex formation between the receptor and CN^- ion, ^{1}H NMR titration experiments were carried out in CD_3OD–d_4. The ^{1}H NMR spectra of **L1** in the absence and presence of various concentrations of cyanide ions are shown in **Figure 3.7**. The ^{1}H NMR spectrum of the receptor **L1** (**Figure 3.7a**) exhibited two sets of peaks, the ferrocene proton appeared about 4.01–4.27 ppm and aromatic proton appeared as three unsymmetrical peak about 7.16–7.49 ppm. Upon addition of incremental amounts of cyanide ions to the solution of **L1** (**Figure 3.7b–3.7e**).

The proton signal of the H_e and H_f combined together and the small upfield shift observed for the aromatic proton, when 1 equiv. of CN^- was added. In addition, when more than 2 equiv. of CN^- was added to solutions of **L1** resulted in the symmetrical peak of the aromatic proton. This observation support the results from cyclic voltammetry.

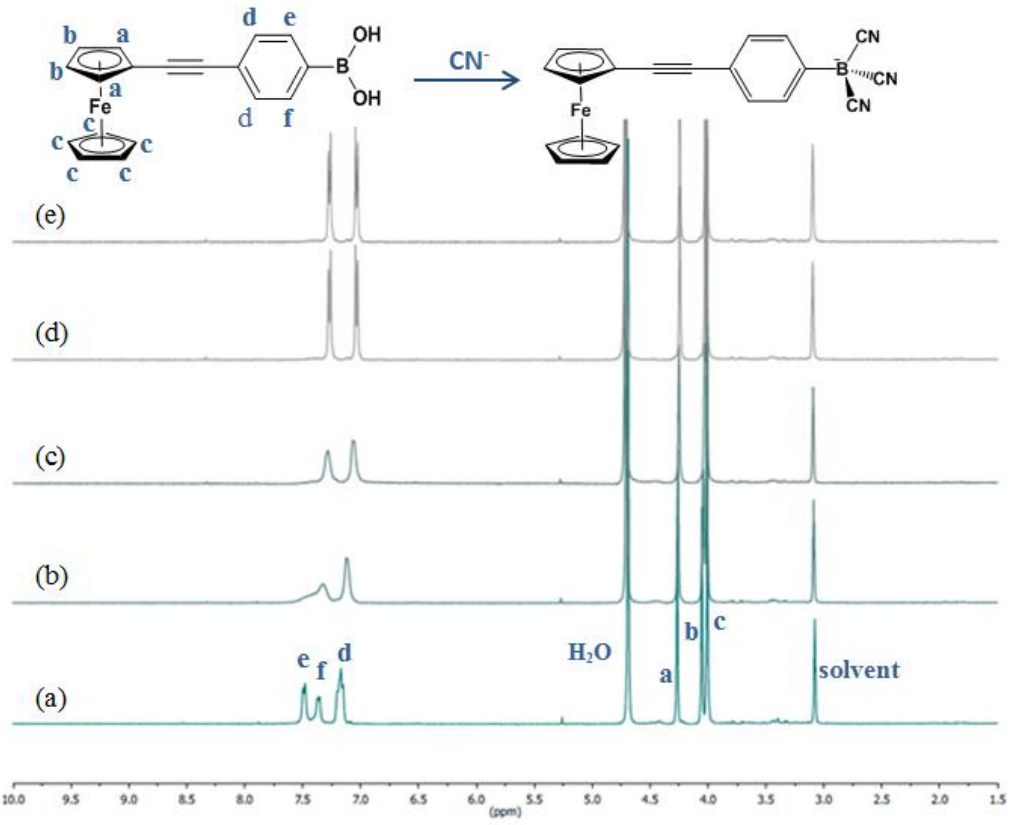

Figure 3.7 ^{1}H NMR spectra of **L1** (1 mM) upon titration with CN^- (0.0–5.0 equiv.) (a) 0 equiv., (b) 0.5 equiv., (c) 1.0 equiv., (d) 2.0 equiv., (e) 5.0 equiv. in CD_3OD.

3.5 Electrochemical studies of L2

3.5.1 Electrochemical studies of L2 with various cations

The electrochemical data of **L2** containing the ferrocene as sensory unit and 2,2'-dipicolylamine (DPA) as receptor unit were investigated using cyclic voltammetry

(CV) in 10% CH_2Cl_2/CH_3CN using 0.1 M $TBAPF_6$ as the supporting electrolyte at a scan rate of 50 mV/s. The cyclic voltammogram of **L2** exhibited three oxidation peaks at 0.22 V, 0.68 V and 1.00 V during the anodic scan as shown in **Figure 3.8**. The regular one-electron reversible wave at 0.22 V vs $Ag/AgNO_3$ was assigned to the Fc/Fc^+ redox couple and two irreversible oxidation peaks at 0.68 V and 1.00 V were probably attributed to N-pyridyl and N-arylamine groups in 2,2'-dipicolylamine (DPA) moiety [48].

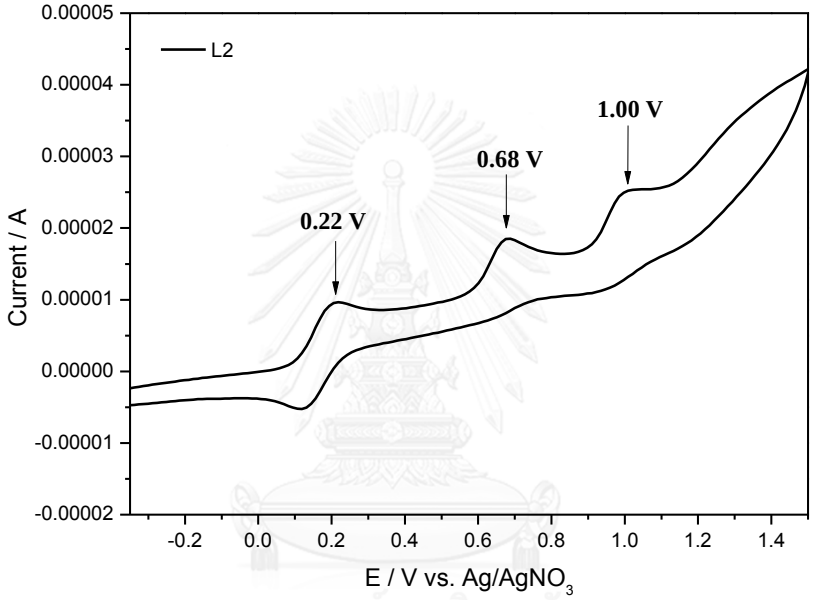

Figure 3.8 Cyclic voltammogram of **L2** (1 mM in 10% CH_2Cl_2/CH_3CN with 0.1 M $TBAPF_6$) at a scan rate of 50 mV/s in the region of -0.2 V to 1.4 V.

The complexation of **L2** with metal ions were studied by cyclic voltammetry (**Figure 3.9**). It was found that only the addition of Cu^{2+} ion caused a new reversible wave of a Cu^{II}/Cu^{I} oxidation peaks at 0.12 V. The ferrocene group in **L2** showing the reversible peak of Fc/Fc^+ redox couple shifted to a more positive potential, from 0.22 V to 0.28 V. In addition, the irreversible oxidation peaks at 0.68 V and 1.00 V of the DPA moiety disappeared upon the gradual addition of Cu^{2+} ion, indicating the coordination of N-DPA to Cu^{2+} ion. The anodic shift of the Fc/Fc^+ redox couple

indicates that electron transfer from the ferrocene to acceptor is less favorable upon complexation with Cu^{2+} ion.

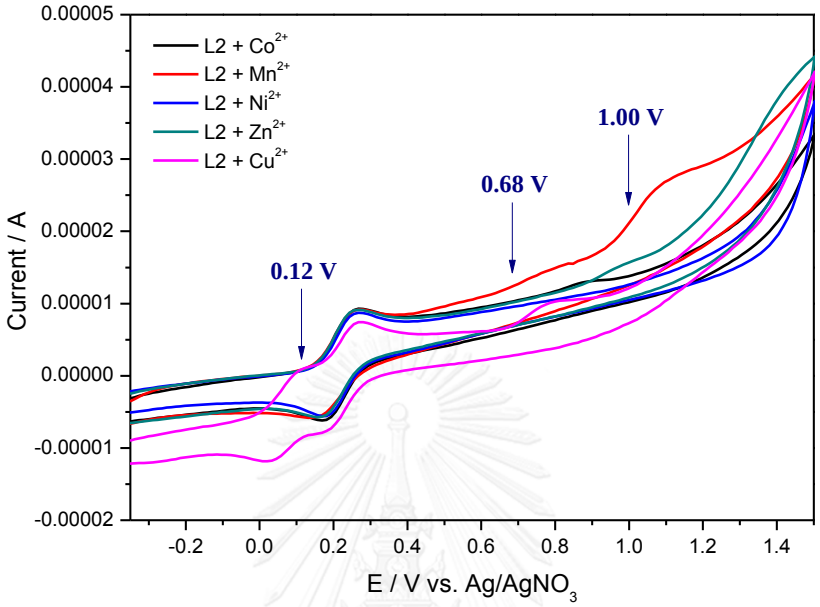

Figure 3.9 Cyclic voltammogram of **L2** (1 mM in 10% CH_2Cl_2/CH_3CN with 0.1 M $TBAPF_6$) in the presence of 1.0 equiv. of different cations (0.01M) at a scan rate of 50 mV/s in the region of -0.2 V to 1.4 V.

3.5.2 Electrochemical titration of L2 with copper (II) ion

The electrochemical property of **L2** upon addition of 0-1.5 equiv. of $Cu(ClO_4)_2$ to the solution of **L2** in 10% CH_2Cl_2/CH_3CN with 0.1 M $TBAPF_6$ at a scan rate of 50 mV/s can be studied by CV titration as shown in **Figure 3.10**. The gradual addition of copper (II) ion to the solution of **L2** caused the anodic shift of Fc/Fc^+ and a new reversible wave of Cu^{II}/Cu^{I} redox couple appeared in the voltammogram. In addition, the change of the redox couples of DPA moiety signified that Cu^{2+} interacted with **L2** in the DPA cavity.

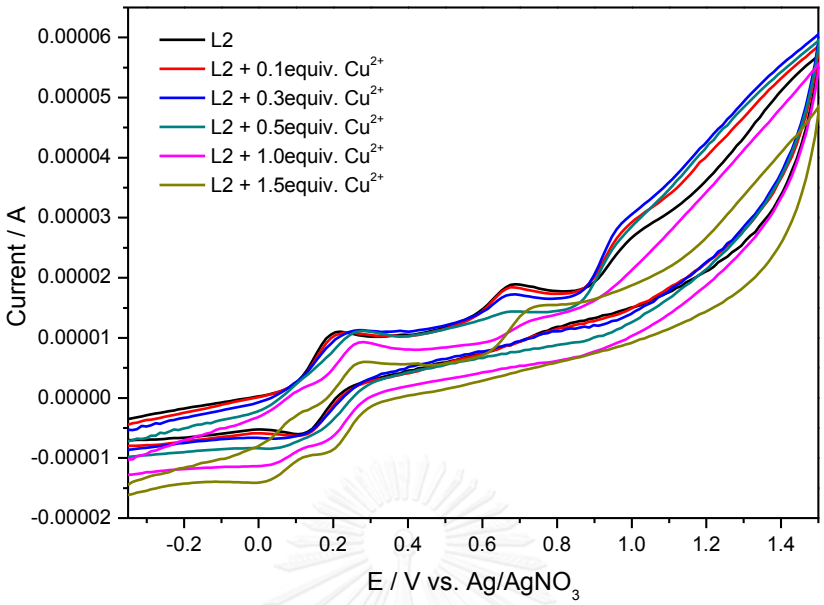

Figure 3.10 Cyclic voltammogram of **L2** (1 mM in 10% CH_2Cl_2/CH_3CN with 0.1 M $TBAPF_6$) upon gradual addition of $Cu(ClO_4)_2$ (0.0-1.5 equiv.) at a scan rate of 50 mV/s in the region of -0.2 V to 1.4 V.

3.6 UV-Vis spectrophotometry and electrochemical studies of L2

3.6.1 UV-Vis spectrophotometry studies of L2 with copper (II) ion

In UV-Vis absorption measurements, **L2** exhibited strong absorption at 310 nm and shoulder peak at 268 nm. Upon addition of Cu^{2+} appeared a large blue shift of the charge transfer band and produced two charge transfer band around 350-420 nm as shown in **Figure 3.11**. In addition, a weaker band at around 420 nm in visible region was assigned to a lower energy produced by a d-d transition of Fe(II) center, or a metal-ligand charge transfer (MLCT) process (d_π-π^*) (LE band) [49, 50]. Therefore, **L2** showed a good interact ion with Cu^{2+} agreeing with the results from cyclic voltammetry.

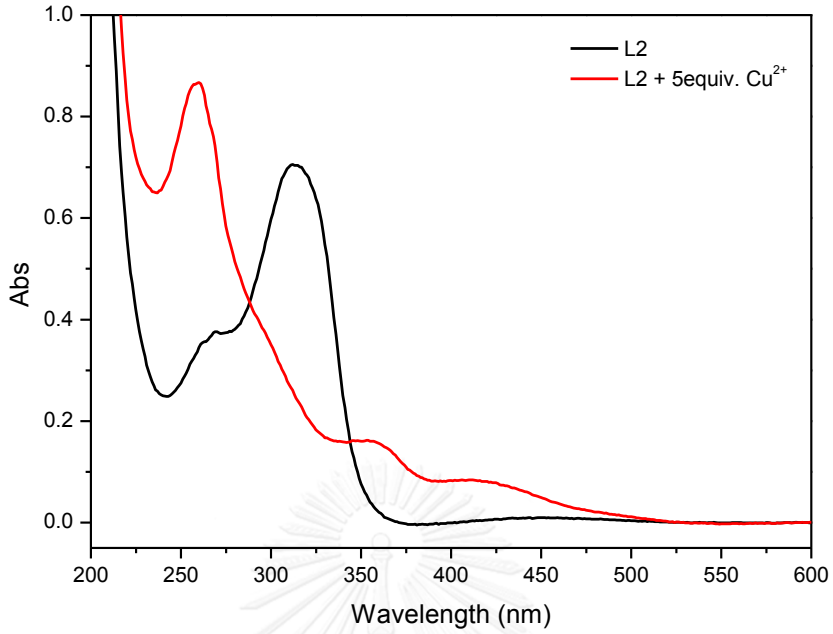

Figure 3.11 Absorption spectra of **L2** (25 μM in CH_3CN) in the presence of 5.0 equiv. of Cu^{2+}.

The UV-Vis response of **L2** with various concentration of Cu^{2+} was also studied as shown in **Figure 3.12**. Interestingly, the UV-Vis spectrum exhibits two step changes, where the first step change took place when Cu^{2+} added to **L2** was less than 1 equiv. As shown in red line, appeared absorptions around 260, 300 and 500 nm appeared in the spectrum. When excess Cu^{2+} was added, the change was observed in blue line and green line. Considering the spectral changes, the addition of more than 1.0 equiv. Cu^{2+} to the solution of **L2** resulted in a blue shift of the CT band and two CT bands at 350 nm and 420 nm appeared as shown in **Figure 3.12**. The coordination of the Cu^{2+} with 2,2'-dipicolylamine (DPA) ligand induced D-A deconjugation process [51], which blocked the ICT process. Resulting in a blue shift in absorption spectra.

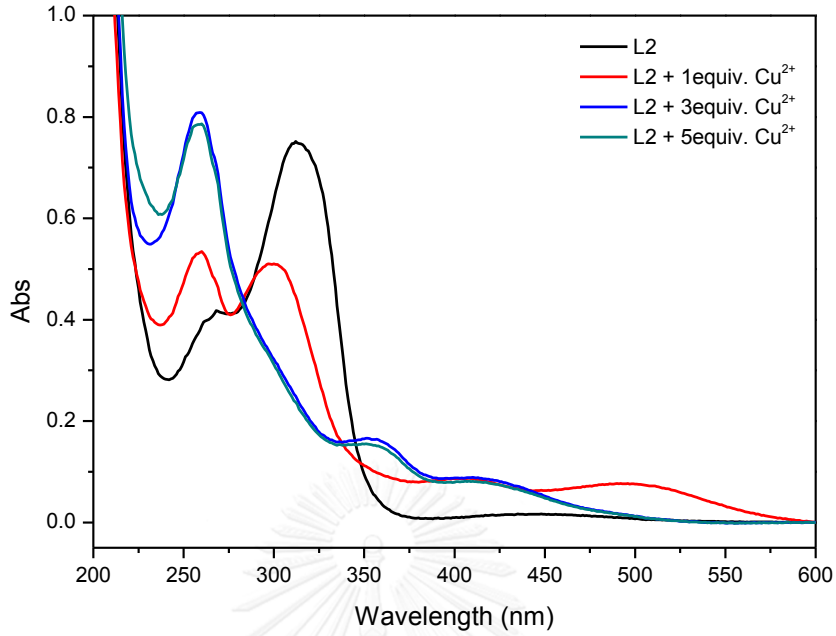

Figure 3.12 Absorption spectra of **L2** (25 μM in CH_3CN) upon gradual addition of $Cu(ClO_4)_2$ (0.0-5.0 equiv.).

3.6.2 UV-Vis spectrophotometry studies of L2-Cu^{2+} in the presence of various anions

The ability of **L2**-Cu^{2+} to interact with various anions at room temperature were explored using UV-Vis spectrophotometry as shown in **Figure 3.13**. Only addition of CN^-, $H_2PO_4^-$ and F^- ion to the solution of **L2**-Cu^{2+} led to the change in absorption spectra by showing a red-shift of the CT band from 260 nm to 310 nm, as shown in **Figure 3.14**. Addition of other anions resulted in small change of the spectrum of **L2**-Cu^{2+}. To investigate the electrochemical property of **L2**-Cu^{2+} in the presence of CN^-, $H_2PO_4^-$ and F^-, the cyclic voltammetry was carried out in 10% CH_2Cl_2/CH_3CN with 0.1 M $TBAPF_6$ at a scan rate of 50 mV/s.

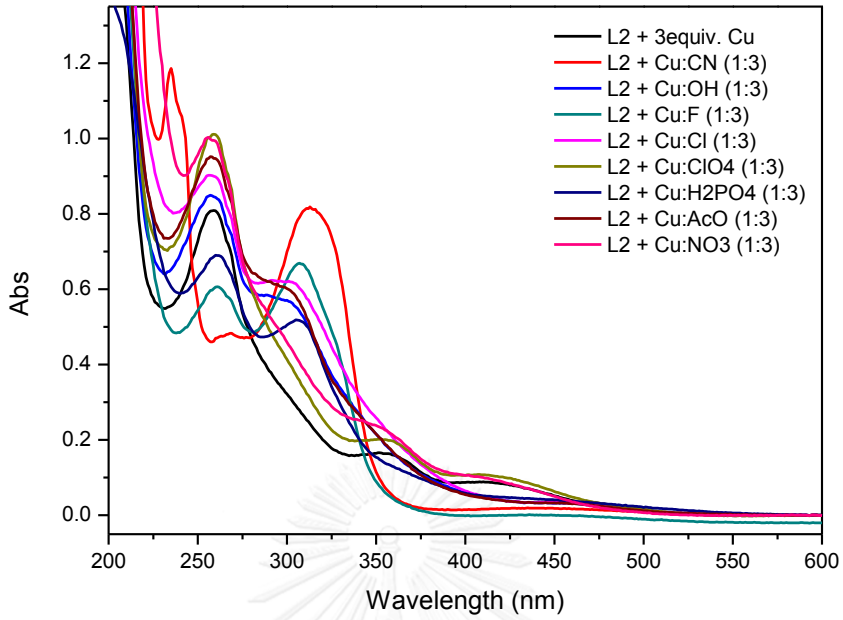

Figure 3.13 Absorption spectra of **L2** (25 μM in CH_3CN) upon addition of 3.0 equiv. of $Cu(ClO_4)_2$ ion and 3.0 equiv. of different anions.

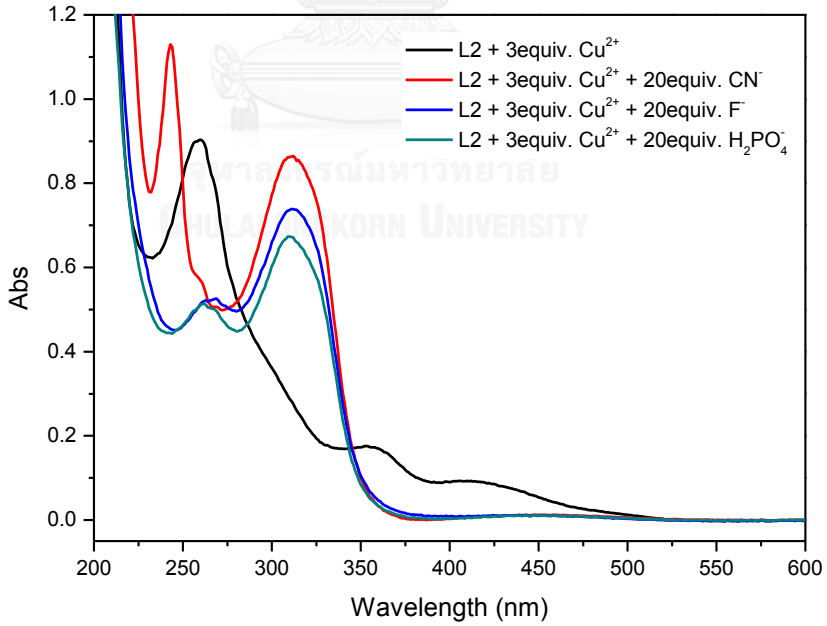

Figure 3.14 Absorption spectra of **L2** (25 μM in CH_3CN) upon addition of 3.0 equiv. of $Cu(ClO_4)_2$ ion and 20.0 equiv. of different anion.

3.6.3 Electrochemical studies of L2-Cu^{2+} in the presence of various anions

According to the results described in UV-Vis studies, the addition of CN^-, F^- and $H_2PO_4^-$ to the solution of **L2** resulted in changes of absorption spectra over other anions. To understand the binding property of receptor **L2** towards CN^-, F^- and $H_2PO_4^-$ under electrochemical condition, cyclic voltammogram of **L2** was mornitored after the addition of these anions to the solution of **L2**-Cu^{2+} complex in 10% CH_2Cl_2/CH_3CN with 0.1 M $TBAPF_6$ at a scan rate of 50 mV/s. The addition of CN^- or F^- 1 equiv. to the solution of cobound [**L2**-Cu^{2+}] complex did not show any redox potential shift of the Fc/Fc^+ and still remained reversible peak (**Figure 3.15 and Figure 3.16**). However, the reversible peak Cu^{II}/Cu^{I} redox couple disappeared, indicating that CN^- and F^- interacted at copper(II) center of **L2**-Cu^{2+} complex. For $H_2PO_4^-$ sensing, after addition of $H_2PO_4^-$ to the solution of cobound [**L2**-Cu^{2+}] complex show the precipitation and show voltammogram in **Figure 3.17**. Therefore, **L2**-Cu^{2+} complex can not use for detection of $H_2PO_4^-$ by using cyclic voltammetry.

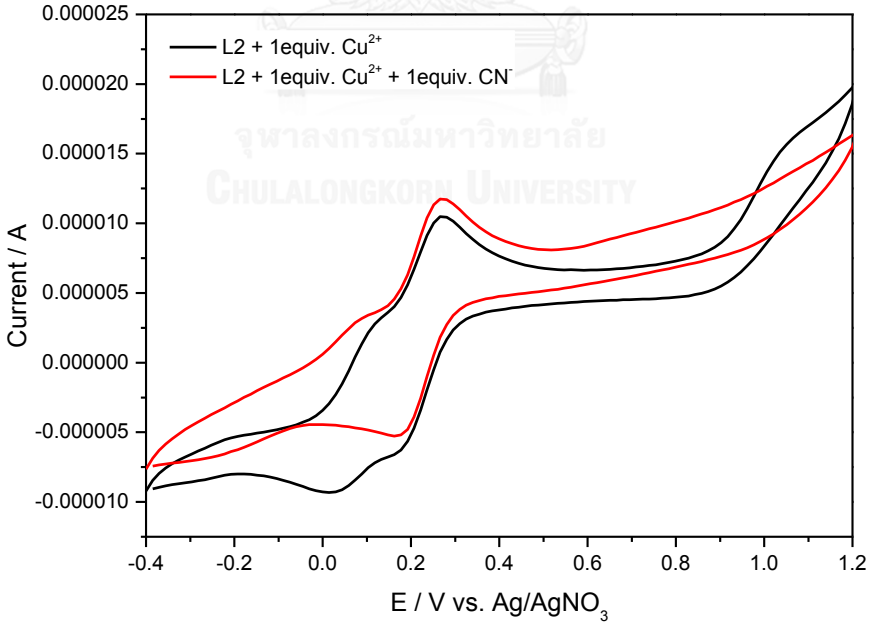

Figure 3.15 Cyclic voltammogram of **L2** (1 mM in 10% CH_2Cl_2/CH_3CN with 0.1 M $TBAPF_6$) upon addition of 1.0 equiv. of $Cu(ClO_4)_2$ ion and 1.0 equiv. of cyanide anion at a scan rate of 50 mV/s in the region of -0.2 V to 1.4 V.

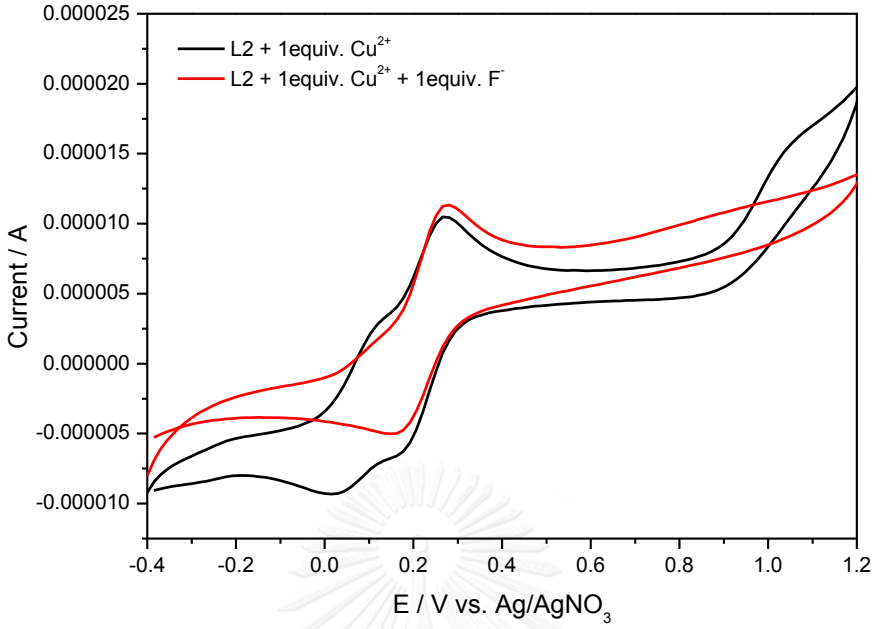

Figure 3.16 Cyclic voltammogram of **L2** (1 mM in 10% CH_2Cl_2/CH_3CN with 0.1 M $TBAPF_6$) upon addition of 1.0 equiv. of $Cu(ClO_4)_2$ ion and 1.0 equiv. of fluoride anion at a scan rate of 50 mV/s in the region of -0.2 V to 1.4 V.

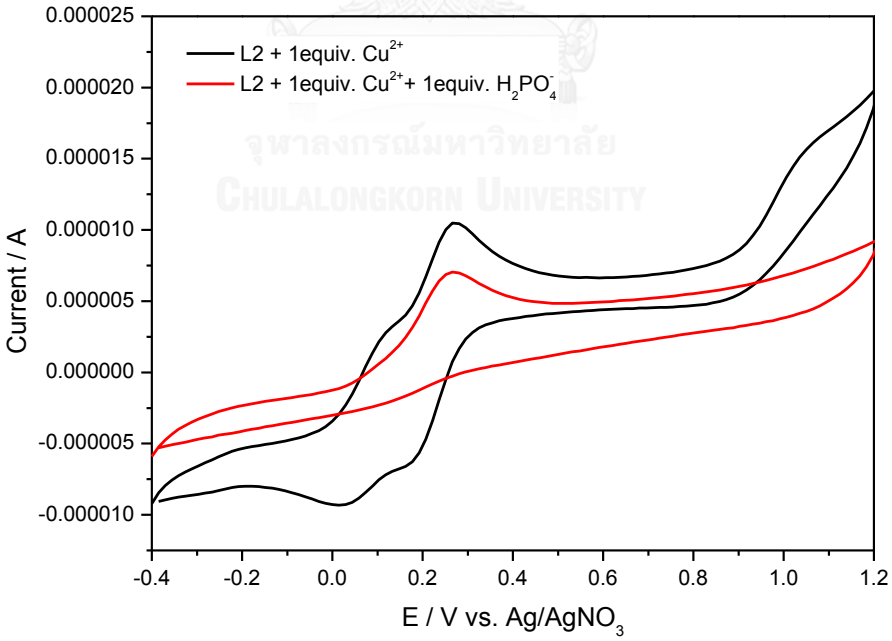

Figure 3.17 Cyclic voltammogram of **L2** (1 mM in 10% CH_2Cl_2/CH_3CN with 0.1 M $TBAPF_6$) upon addition of 1.0 equiv. of $Cu(ClO_4)_2$ ion and 1.0 equiv. of dihydrogen phosphate anion at a scan rate of 50 mV/s in the region of -0.2 V to 1.4 V.

3.7 DFT studies of L2-Cu^{2+} in the presence of CN^- and F^-

In this study, we are interested in the structure of the **L2**-Cu^{2+} complexes with CN^- and F^- ions. The optimized geometries are calculated by using the DFT(B3LYP) methods with LANL2DZ basis sets. The result of **L2**-Cu^{2+} in the presence of CN^- is shown in **Figure 3.18**. The eclip conformation of cyclopentadienyl is clearly seen in **Figure 3.18a**. From **Figure 3.18b** it is found that cyclopentadienyl, triple bond and phenyl group of this structure are in the same plain indicating a good π-conjugate. Moreover, **Figure 3.18c** shows that N-atom of DPA moiety and C-atom of CN^- ion co-ordinate to Cu^{2+} center. In the case of F^- ion, the Cu^{2+} center has a similar geometry as found in CN^-. The result in **Figure 3.19** shows that F^- co-ordinate directly to Cu^{2+} center. In addition, the calculation results indicated some selected bond length values for the **L2**-Cu^{2+} complex in the presence of CN^- and F^- ions. The bond lengths between Cu^{2+} and N-DPA from reference data of similar crystal structure [52] and our DFT calculation are compared in **Table 3.1**. The bond lengths of N-arylamine from reference are shorter than our calculated data. Therefore, the coordination of CN^- and F^- ions at the Cu^{2+} center resulted in a weaker bond between Cu^{2+} and N-arylamine on DPA moiety. The results agree with the result from UV-Vis spectrophotometry and cyclic voltammetry.

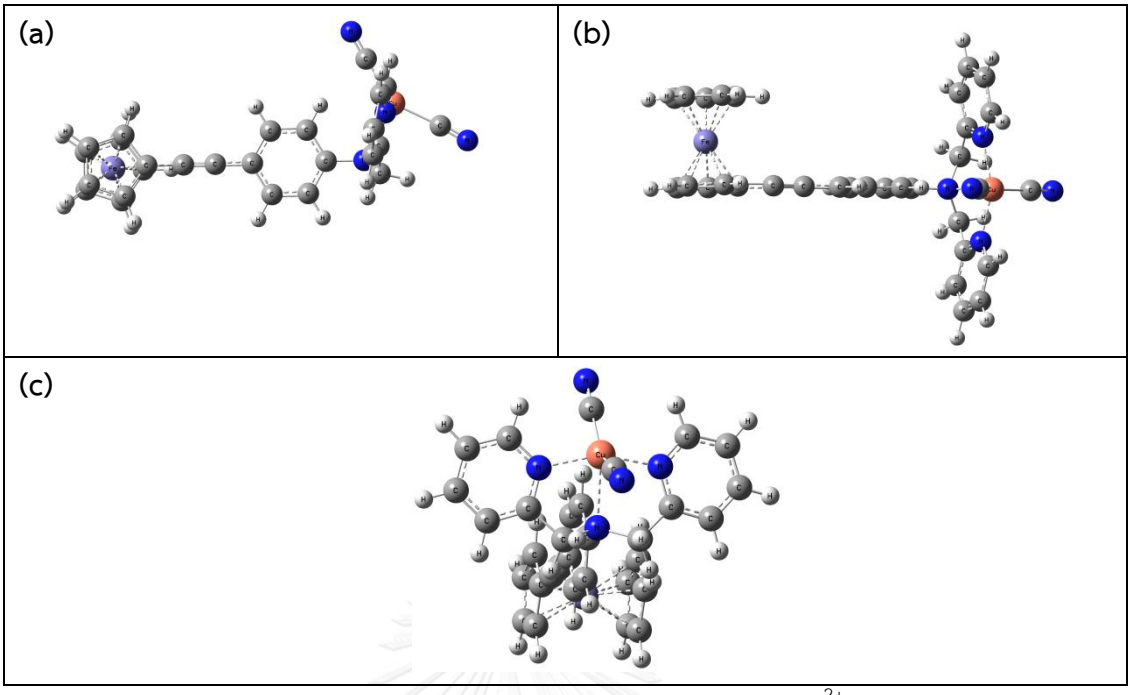

Figure 3.18 B3LYP/LANL2DZ-optimized structure of the **L2**-Cu^{2+}-CN^{-} **a)** side view **b)** top view **c)** top view.

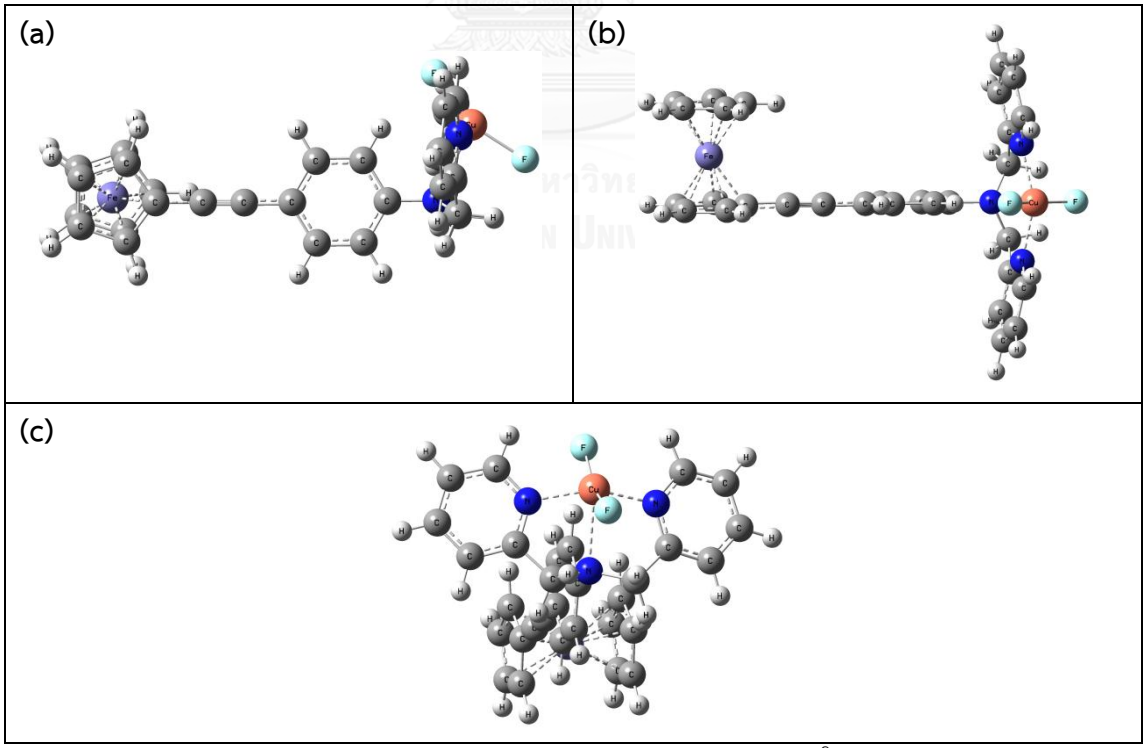

Figure 3.19 B3LYP/LANL2DZ-optimized structure of the **L2**-Cu^{2+}-F^{-} **a)** side view **b)** top view **c)** top view.

Table 3.1 Geometrical parameters optimized for **L2**-Cu^{2+}-CN^{-} and **L2**-Cu^{2+}-F^{-}, some selected bond lengths (A°)

Bond definition	Optimized Parameters of crystal structure (A°) [50]	Optimized parameters of **L2**-Cu^{2+}-CN^{-} (A°)	Optimized parameters of **L2**-Cu^{2+}-F^{-} (A°)
$Cu\text{-}N_{piridyl}$	1.990 (S.D. = 0.018)	2.065	2.026
$Cu\text{-}N_{arylamine}$	2.104 (S.D. = 0.032)	2.455	2.482
Cu-CN	-	2.008	-
Cu-F	-	-	1.900

CHAPTER IV

CONCLUSION

The synthesis of ferrocene derivatives containing aryl ethyne spacer and ferrocene moiety as redox–active unit have been accomplished (**L1** and **L2**). The compounds have been successfully synthesized by the Pd/Cu catalyzed Sonogashira coupling to obtain desired products **L1** (45% yield) and **L2** (67% yield). The products were characterized by ^{1}H and ^{13}C NMR spectroscopy, MALDI–TOF mass spectrometry and elemental analysis. Compound **L1** possessing boronic acid as a receptor unit, exhibited high selectivity toward cyanide ions in the presence of halides and other common anions using cyclic voltammetry in CH_3CN with 0.1 M $TBAPF_6$. Cyanide ion binding event occurring at the boronic acid site can be detected by ^{1}H NMR titration. Therefore, **L1** is a potential electrochemical sensor for cyanide anion. Compound **L2** possessing 2, 2-dipicolylamine as receptor unit can recognize Cu^{2+} selectively. The electrochemical property of **L2** toward Cu^{2+} in 10% CH_2Cl_2/CH_3CN with 0.1 M $TBAPF_6$, the gradual addition of Cu^{2+} ion to the solution of **L2** exhibited anodic shift of Fc/Fc^{+} and appeared a new reversible wave of Cu^{II}/Cu^{I} redox couple. In addition, the DPA moiety disappeared indicating that Cu^{2+} interacted with **L2** at DPA carvity. The addition of Cu^{2+} to the solution of **L2** led to a blue shift of the absorption band from 310 nm to 260 nm. The addition of CN^{-}, $H_2PO_4^{-}$ and F^{-} ion to the solution of **L2**-Cu^{2+} led to the change in absorption spectra by showing a red shift in the absorption band from 260 nm to 310 nm. The shift in absorption of **L2**-Cu^{2+} suggested the binding of Cu^{2+} with these anions (CN^{-}, $H_2PO_4^{-}$ and F^{-}). Addition of 1 equiv. of CN^{-} and F^{-} to the solution of **L2**-Cu^{2+} complex did not show any redox potential shift of the Fc/Fc^{+} and the Cu^{II}/Cu^{I} redox couple disappeared, indicating that CN^{-} and F^{-}

interacted at copper (II) center of **L2**-Cu^{2+} complex. In addition, DFT studies suggested that the coordination of CN^- and F^- ions to the Cu^{2+} center resulted in a weaker bond between Cu^{2+} and N-arylamine on the DPA moiety.

REFERENCES

[1] Bhardwaj, S. and Singh, A.K. Visual & amp; reversible sensing of cyanide in real samples by an effective ratiometric colorimetric probe & amp; logic gate application. Journal of Hazardous Materials 296 (2015): 54-60.

[2] Wang, S., Fei, X., Guo, J., Yang, Q., Li, Y., and Song, Y. A novel reaction-based colorimetric and ratiometric fluorescent sensor for cyanide anion with a large emission shift and high selectivity. Talanta 148 (2016): 229-236.

[3] Chow, C.-F., Lam, M.H.W., and Wong, W.-Y. A Heterobimetallic Ruthenium(II)–Copper(II) Donor–Acceptor Complex as a Chemodosimetric Ensemble for Selective Cyanide Detection. Inorganic Chemistry 43(26) (2004): 8387-8393.

[4] Lou, X., Zhang, L., Qin, J., and Li, Z. An alternative approach to develop a highly sensitive and selective chemosensor for the colorimetric sensing of cyanide in water. Chemical Communications (44) (2008): 5848-5850.

[5] Wang, B., Takahashi, S., Du, X., and Anzai, J.-i. Electrochemical Biosensors Based on Ferroceneboronic Acid and Its Derivatives: A Review. Biosensors 4(3) (2014).

[6] Chen, J., Lalancette, R.A., and Jäkle, F. Chiral Organoborane Lewis Pairs Derived from Pyridylferrocene. Chemistry – A European Journal 20(29) (2014): 9120-9129.

[7] Nishiyabu, R., Kubo, Y., James, T.D., and Fossey, J.S. Boronic acid building blocks: tools for sensing and separation. Chemical Communications 47(4) (2011): 1106-1123.

[8] Lorand, J.P. and Edwards, J.O. Polyol Complexes and Structure of the Benzeneboronate Ion. The Journal of Organic Chemistry 24(6) (1959): 769-774.

[9] Dusemund, C., Sandanayake, K.R.A.S., and Shinkai, S. Selective fluoride recognition with ferroceneboronic acid. Journal of the Chemical Society, Chemical Communications (3) (1995): 333-334.

[10] Swamy, K.M.K., et al. A New Fluorescein Derivative Bearing a Boronic Acid Group as a Fluorescent Chemosensor for Fluoride Ion. The Journal of Organic Chemistry 71(22) (2006): 8626-8628.

[11] Yamaguchi, S., Akiyama, S., and Tamao, K. Colorimetric Fluoride Ion Sensing by Boron-Containing π-Electron Systems. Journal of the American Chemical Society 123(46) (2001): 11372-11375.

[12] Ooyama, Y., Furue, K., Uenaka, K., and Ohshita, J. Development of highly-sensitive fluorescence PET (photo-induced electron transfer) sensor for water: anthracene-boronic acid ester. RSC Advances 4(48) (2014): 25330-25333.

[13] Kim, Y., Huh, H.-S., Lee, M.H., Lenov, I.L., Zhao, H., and Gabbaï, F.P. Turn-On Fluorescence Sensing of Cyanide Ions in Aqueous Solution at Parts-per-Billion Concentrations. Chemistry – A European Journal 17(7) (2011): 2057-2062.

[14] Tirfoin, R. and Aldridge, S. A molecular 'traffic light': highly selective cyanide sensing in aqueous media by a CpFe(indenyl)-functionalized borane. Dalton Transactions 42(36) (2013): 12836-12839.

[15] Bridgeman, A.J., Wilkin, O.M., and Young, N.A. Dinitrogen bonding modes to molecular nickel(II) halides: a matrix isolation IR and DFT study. Inorganic Chemistry Communications 3(12) (2000): 681-684.

[16] Suksai, C. and Tuntulani, T. Chromogenic anion sensors. Chemical Society Reviews 32(4) (2003): 192-202.

[17] Wiskur, S.L., Ait-Haddou, H., Lavigne, J.J., and Anslyn, E.V. Teaching Old Indicators New Tricks. Accounts of Chemical Research 34(12) (2001): 963-972.

[18] Loehr, H.G. and Voegtle, F. Chromo- and fluoroionophores. A new class of dye reagents. Accounts of Chemical Research 18(3) (1985): 65-72.

[19] Beer, P.D. and Bayly, S.R. Anion Sensing by Metal-Based Receptors. in Stibor, I. (ed.)Anion Sensing, pp. 125-162. Berlin, Heidelberg: Springer Berlin Heidelberg, 2005.

[20] Reddy G, U., Das, P., Saha, S., Baidya, M., Ghosh, S.K., and Das, A. A CN-specific turn-on phosphorescent probe with probable application for enzymatic assay and as an imaging reagent. Chemical Communications 49(3) (2013): 255-257.

[21] Chen, H., Liu, Z., Cao, D., Lu, S., Pang, J., and Sun, Y. Two new fluorescence turn-on chemosensors for cyanide based on dipyridylamine and aurone moiety. Sensors and Actuators B: Chemical 199 (2014): 115-120.

[22] Park, G.J., Hwang, I.H., Song, E.J., Kim, H., and Kim, C. A colorimetric and fluorescent sensor for sequential detection of copper ion and cyanide. Tetrahedron 70(17) (2014): 2822-2828.

[23] Goswami, S., Paul, S., and Manna, A. FRET based selective and ratiometric 'naked-eye' detection of CN^- in aqueous solution on fluorescein–Zn–naphthalene ensemble platform. Tetrahedron Letters 55(29) (2014): 3946-3949.

[24] Khajehsharifi, H. and Bordbar, M.M. A highly selective chemosensor for detection and determination of cyanide by using an indicator displacement assay and PC-ANN and its logic gate behavior. Sensors and Actuators B: Chemical 209 (2015): 1015-1022.

[25] Park, G.J., You, G.R., Choi, Y.W., and Kim, C. A naked-eye chemosensor for simultaneous detection of iron and copper ions and its copper complex for colorimetric/fluorescent sensing of cyanide. Sensors and Actuators B: Chemical 229 (2016): 257-271.

[26] Jo, H.Y., Park, G.J., Na, Y.J., Choi, Y.W., You, G.R., and Kim, C. Sequential colorimetric recognition of Cu^{2+} and CN^- by asymmetric coumarin-conjugated naphthol groups in aqueous solution. Dyes and Pigments 109 (2014): 127-134.

[27] Zou, Q., Li, X., Zhang, J., Zhou, J., Sun, B., and Tian, H. Unsymmetrical diarylethenes as molecular keypad locks with tunable photochromism and fluorescence via Cu^{2+} and CN^- coordinations. Chemical Communications 48(15) (2012): 2095-2097.

[28] Park, G.J., Choi, Y.W., Lee, D., and Kim, C. A simple colorimetric chemosensor bearing a carboxylic acid group with high selectivity for CN^-. Spectrochimica Acta Part A: Molecular and Biomolecular Spectroscopy 132 (2014): 771-775.

[29] Huang, X., Guo, Z., Zhu, W., Xie, Y., and Tian, H. A colorimetric and fluorescent turn-on sensor for pyrophosphate anion based on a dicyanomethylene-4H-chromene framework. Chemical Communications (41) (2008): 5143-5145.

[30] Zhang, J.F., et al. Pyrophosphate-Selective Fluorescent Chemosensor Based on 1,8-Naphthalimide–DPA–Zn(II) Complex and Its Application for Cell Imaging. Organic Letters 13(19) (2011): 5294-5297.

[31] Chung, S.-Y., Nam, S.-W., Lim, J., Park, S., and Yoon, J. A highly selective cyanide sensing in watervia fluorescence change and its application to in vivo imaging. Chemical Communications (20) (2009): 2866-2868.

[32] Lee, J.H., Jeong, A.R., Jung, J.-H., Park, C.-M., and Hong, J.-I. A Highly Selective and Sensitive Fluorescence Sensing System for Distinction between Diphosphate and Nucleoside Triphosphates. The Journal of Organic Chemistry 76(2) (2011): 417-423.

[33] Cao, X., Lin, W., and He, L. A Near-Infrared Fluorescence Turn-On Sensor for Sulfide Anions. Organic Letters 13(17) (2011): 4716-4719.

[34] Maldonado, C.R., Touceda-Varela, A., Jones, A.C., and Mareque-Rivas, J.C. A turn-on fluorescence sensor for cyanide from mechanochemical reactions between quantum dots and copper complexes. Chemical Communications 47(42) (2011): 11700-11702.

[35] Das, P., Ghosh, A., Kesharwani, M.K., Ramu, V., Ganguly, B., and Das, A. Zn^{II}–2,2′:6′,2″-Terpyridine-Based Complex as Fluorescent Chemosensor for PPi, AMP and ADP. European Journal of Inorganic Chemistry 2011(20) (2011): 3050-3058.

[36] Fabbrizzi, L., Marcotte, N., Stomeo, F., and Taglietti, A. Pyrophosphate Detection in Water by Fluorescence Competition Assays: Inducing Selectivity through the Choice of the Indicator. Angewandte Chemie International Edition 41(20) (2002): 3811-3814.

[37] Steed, J.W. Coordination and organometallic compounds as anion receptors and sensors. Chemical Society Reviews 38(2) (2009): 506-519.

[38] Helal, A.K., Se-Beom;Kim, Hong-Seok. Sensing of Cyanide Using Highly Selective Thiazole-based Cu^{2+} Chemosensor. Bulletin of the Korean Chemical Society 32(spc8) (2011): 3123-3126.

[39] Xu, J.-F., et al. A colorimetric and fluorometric dual-modal chemosensor for cyanide in water. Sensors and Actuators B: Chemical 168 (2012): 14-19.

[40] Walaijai, K. Synthesis of aryl ethyne derivatives containing various receptors as anion sensors. Master's degree, 2013 Chulalongkorn University.

[41] Yamamoto, H., Ori, A., Ueda, K., Dusemund, C., and Shinkai, S. Visual sensing of fluoride ion and saccharides utilizing a coupled redox reaction of ferrocenylboronic acids and dye molecules. Chemical Communications (3) (1996): 407-408.

[42] Cooper, C.R., Spencer, N., and James, T. D. Selective fluorescence detection of fluoride using boronic acids. Chemical Communications (13) (1998): 1365-1366.

[43] Yamaguchi, S., Akiyama, S., and Tamao, K. Photophysical Properties Changes Caused by Hypercoordination of Organosilicon Compounds: From Trianthrylfluorosilane to Trianthryldifluorosilicate. Journal of the American Chemical Society 122(28) (2000): 6793-6794.

[44] Nicolas, M., Fabre, B., and Simonet, J. Boronate-functionalized polypyrrole as a new fluoride sensing material. Chemical Communications (18) (1999): 1881-1882.

[45] Frisch, M.J., et al. Gaussian 09 Revision D.01. Gaussian Inc Wallingford, CT., 2014.

[46] Dennington, R., Keith, T., and Millam, J. GaussView, Version 5. Semichem Inc. Shawnee Mission, KS, 2009.

[47] Cuffe, L., et al. Synthesis, Structure, and Redox Chemistry of Ethenyl and Ethynyl Ferrocene Polyaromatic Dyads. Organometallics 24(9) (2005): 2051-2060.

[48] Plenio, H. and Burth, D. Aminoferrocenes and Aminocobaltocenes as Redox-Active Chelating Ligands: Syntheses, Structures, and Coordination Chemistry1. Organometallics 15(19) (1996): 4054-4062.

[49] Molina, P., Tárraga, A., and Caballero, A. Ferrocene-Based Small Molecules for Multichannel Molecular Recognition of Cations and Anions. European Journal of Inorganic Chemistry 2008(22) (2008): 3401-3417.

[50] Erdemir, S., Deveci, P., Taner, B., and Kocyigit, O. Synthesis and electrochemical properties of calix[4]arene derivatives containing ferrocene units in the cone and 1,3-alternate conformation. Tetrahedron 68(2) (2012): 642-646.

[51] Yang, J.-S., Lin, Y.-D., Lin, Y.-H., and Liao, F.-L. Zn(II)-Induced Ground-State π-Deconjugation and Excited-State Electron Transfer in N,N-Bis(2-pyridyl)amino-Substituted Arenes. The Journal of Organic Chemistry 69(10) (2004): 3517-3525.

[52] Osako, T., et al. Quantitative Evaluation of d–π Interaction in Copper(I) Complexes and Control of Copper(I)–Dioxygen Reactivity. Chemistry – A European Journal 10(1) (2004): 237-246.

APPENDIX

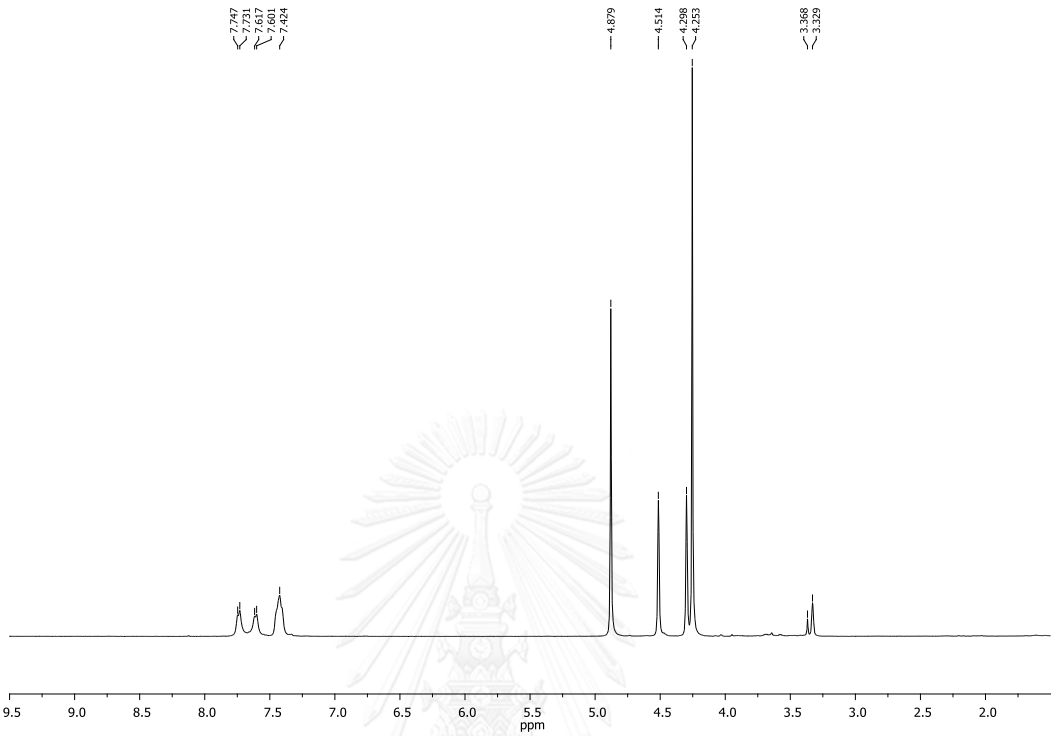

Figure A1 ^{1}H NMR spectrum of **L1** in CD_3OD.

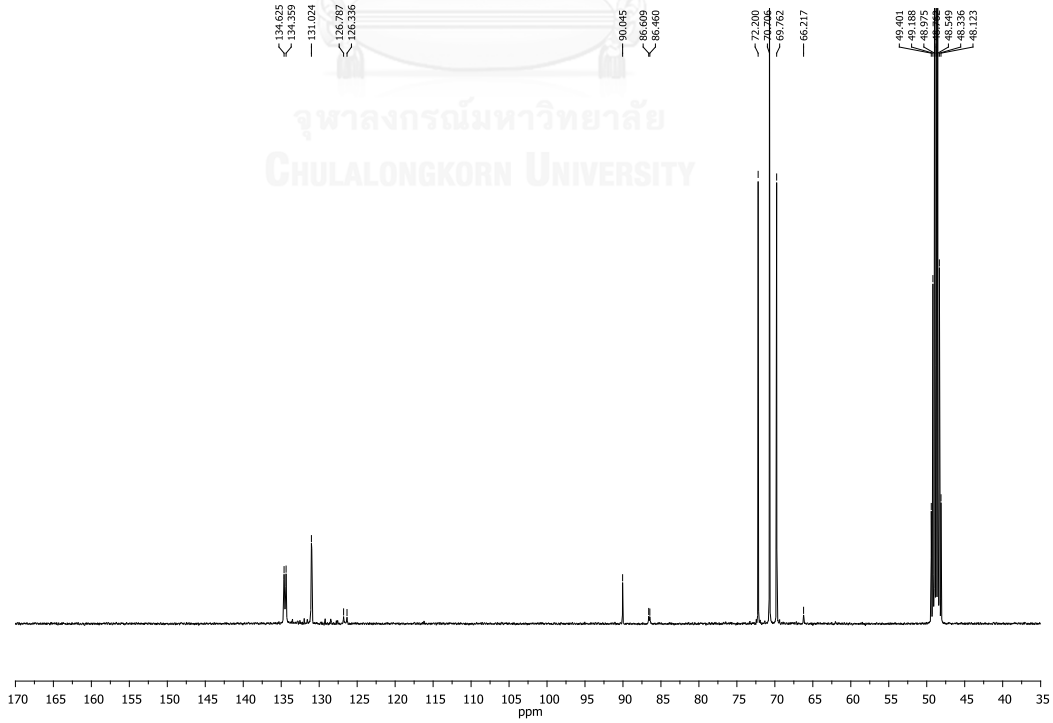

Figure A2 ^{13}C NMR spectrum of **L1** in CD_3OD.

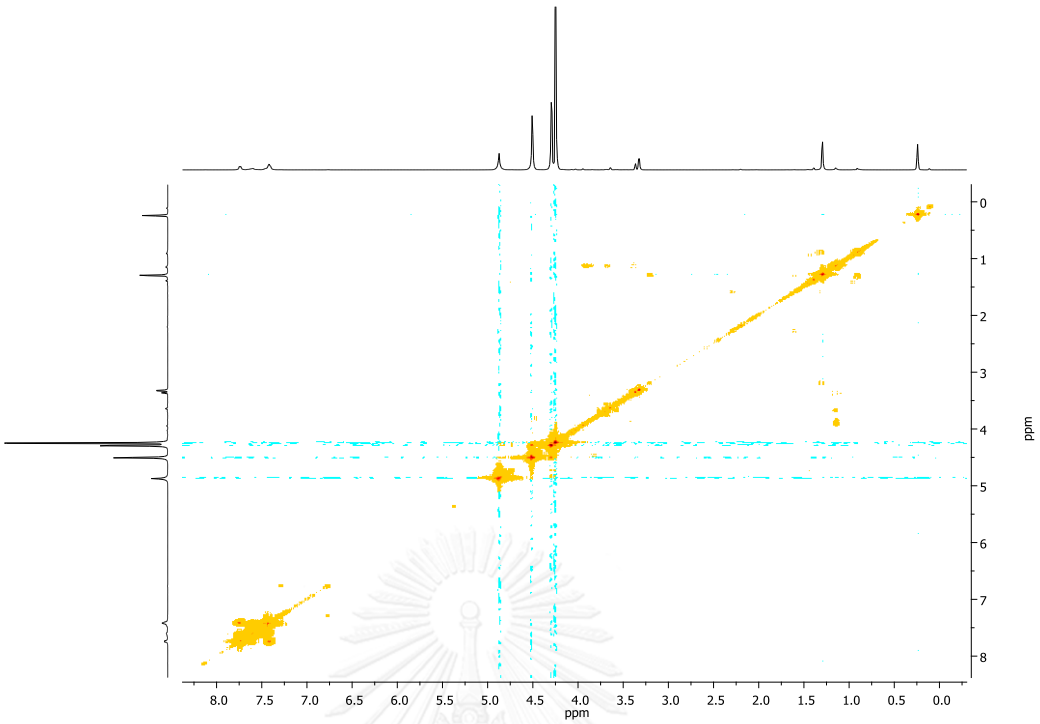

Figure A3 COSY spectrum of **L1** in CD_3OD.

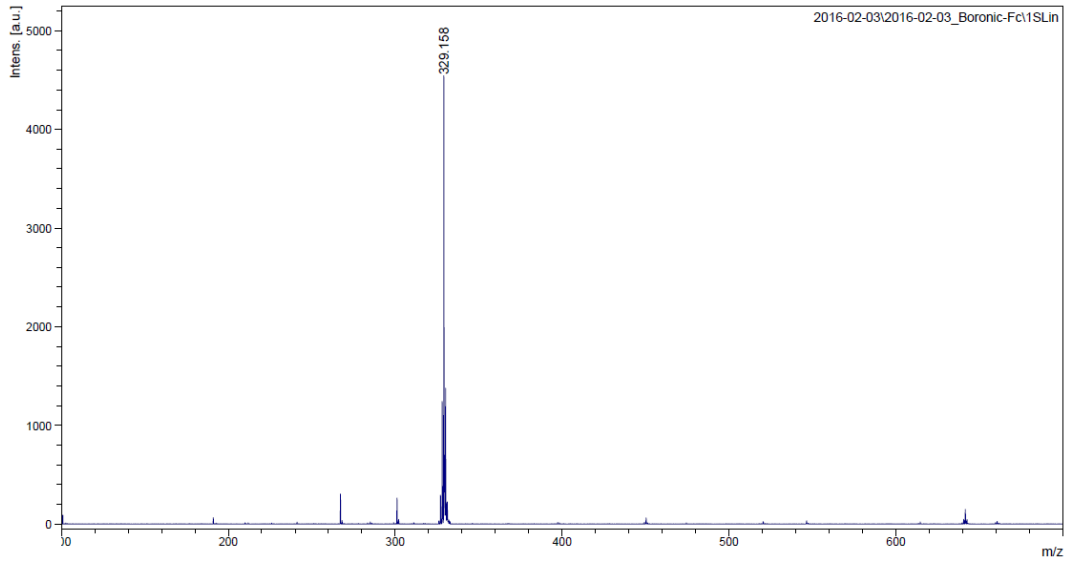

Figure A4 MALDI-TOF mass spectrum of **L1**.

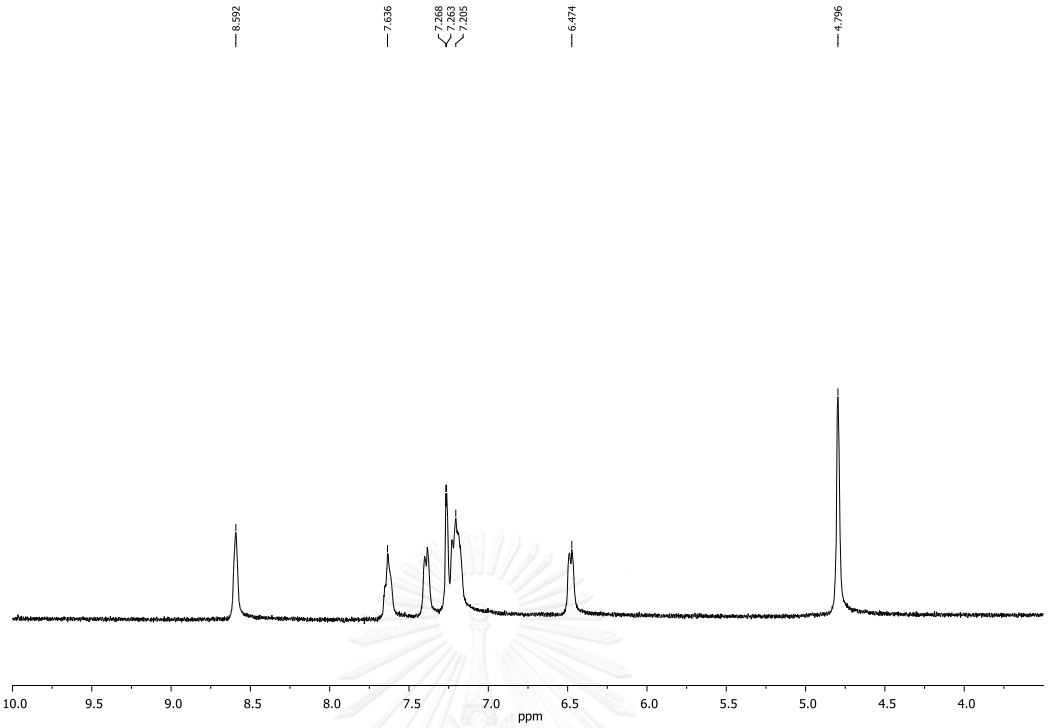

Figure A5 ^{1}H NMR spectrum of **2a** in CD_3Cl.

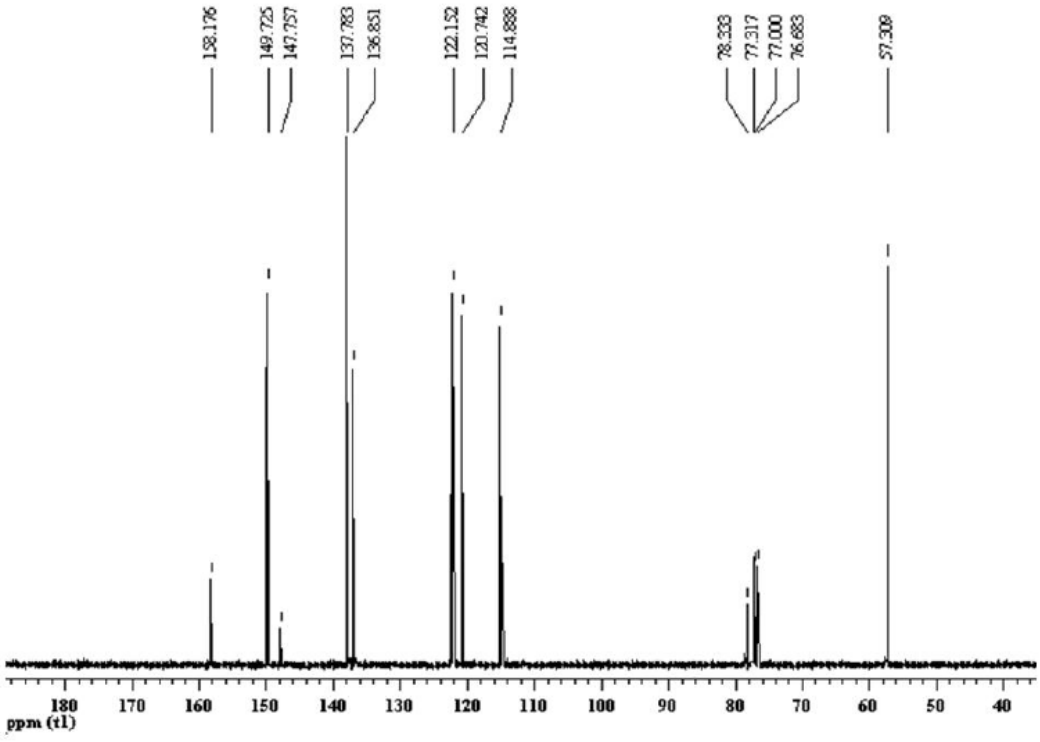

Figure A6 ^{13}C NMR spectrum of **2a** in CD_3Cl.

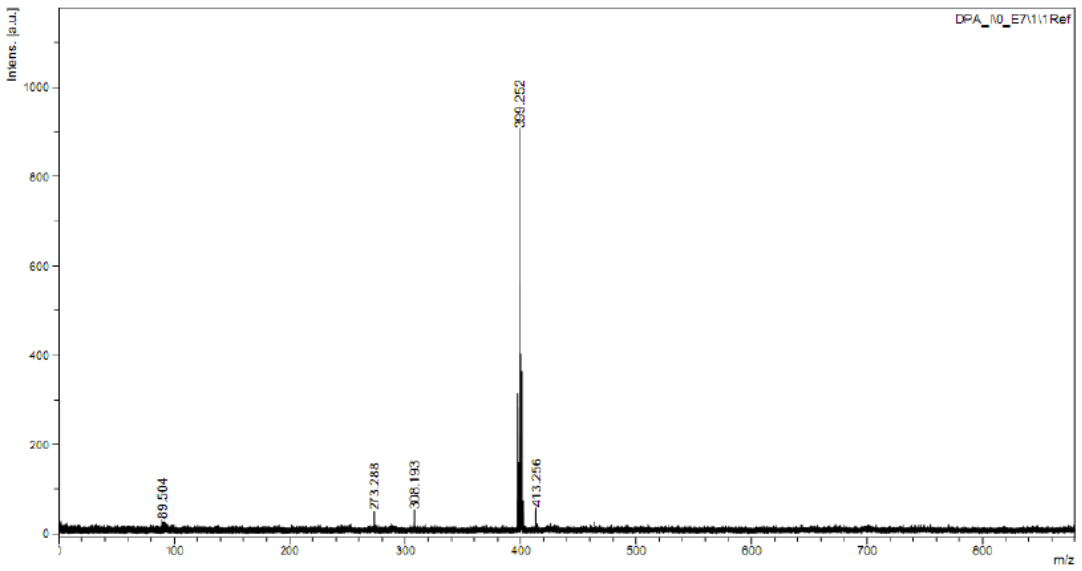

Figure A7 MALDI-TOF mass spectrum of **2a**.

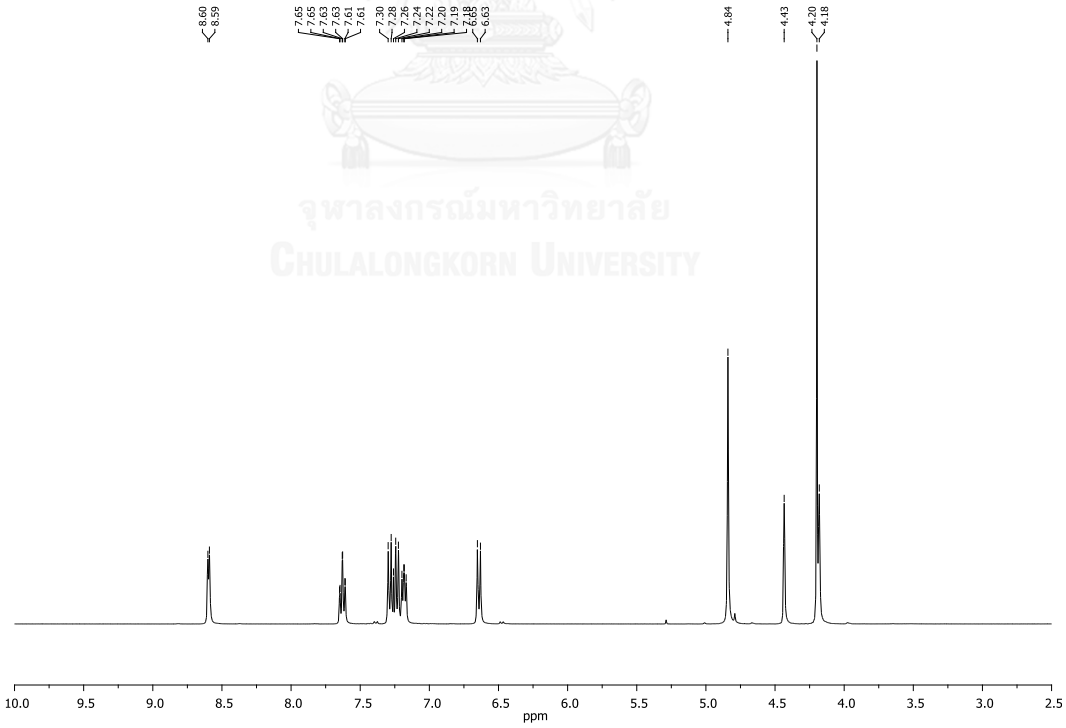

Figure A8 ^{1}H NMR spectrum of **L2** in CD_3Cl.

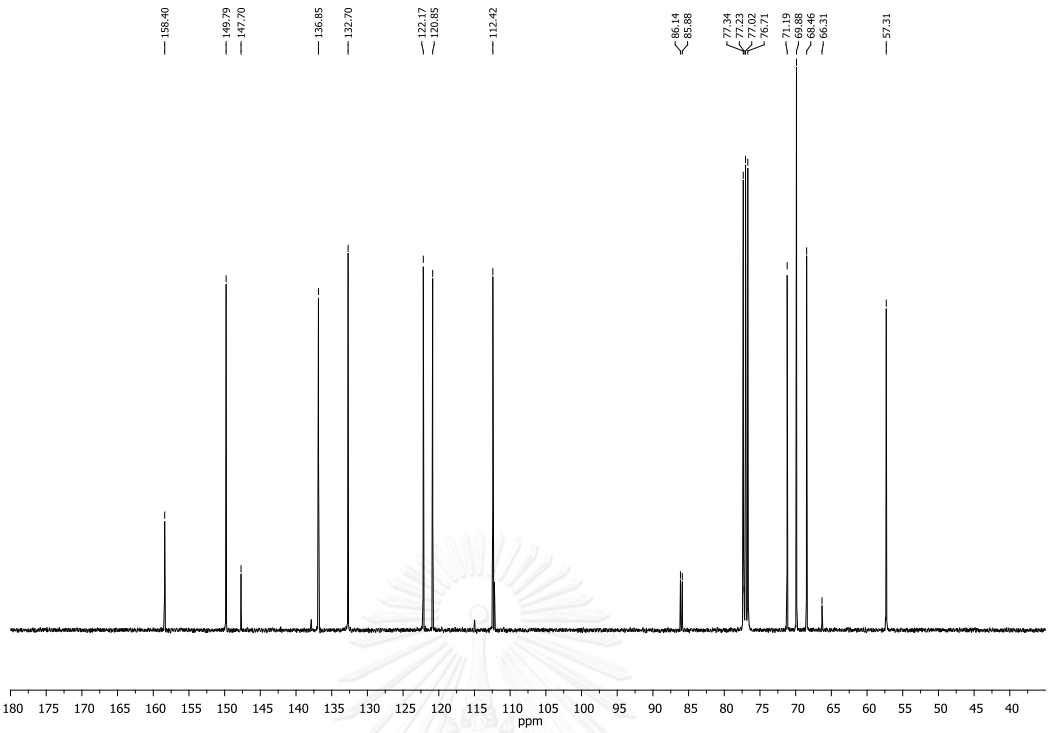

Figure A9 ^{13}C NMR spectrum of **L2** in CD_3Cl.

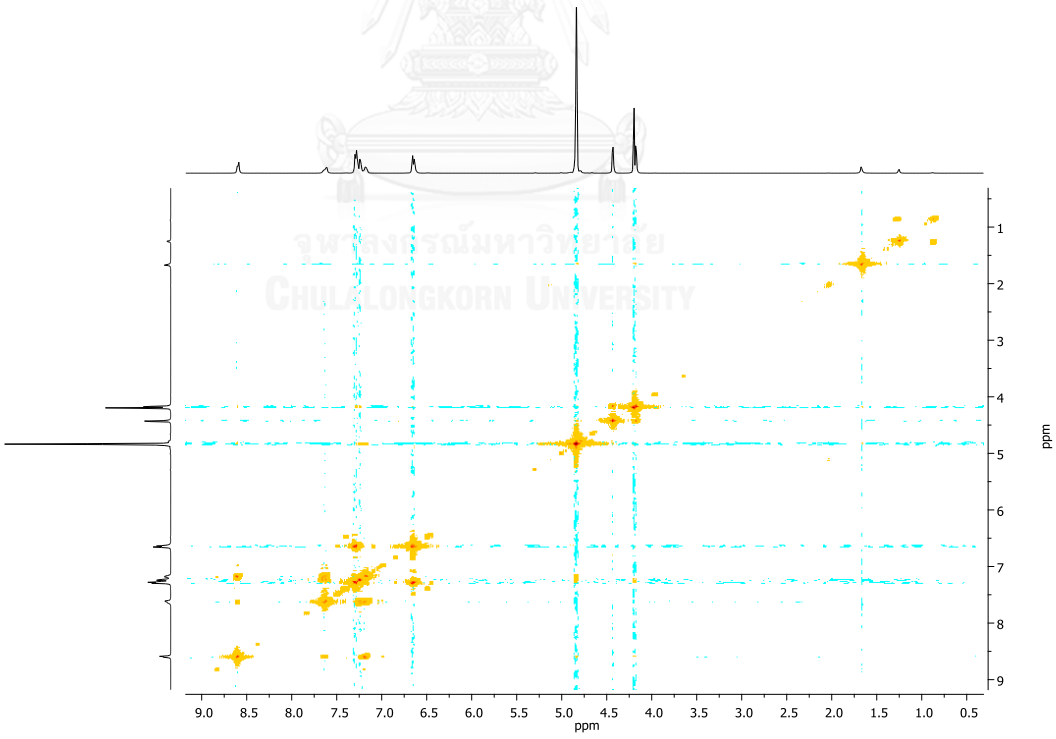

Figure A10 COSY spectrum of **L2** in CD_3Cl.

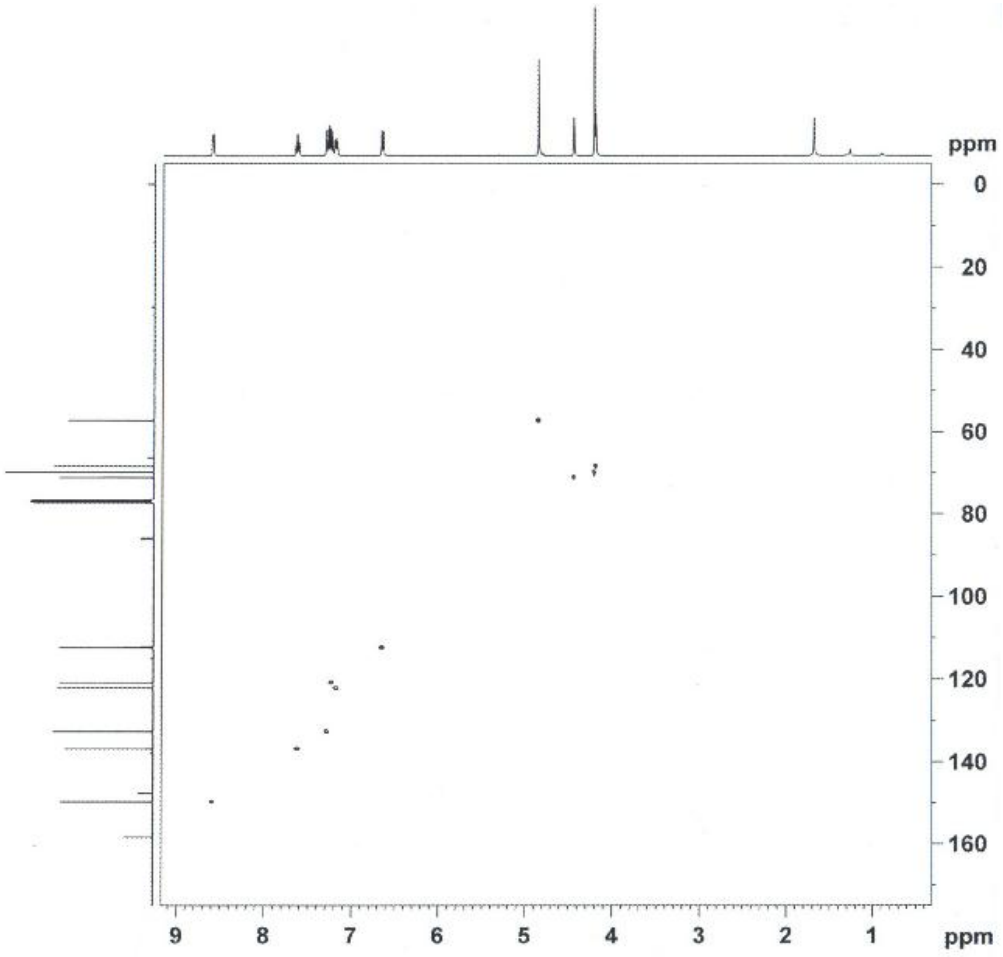

Figure A11 HSQC spectrum of **L2** in CD_3Cl.

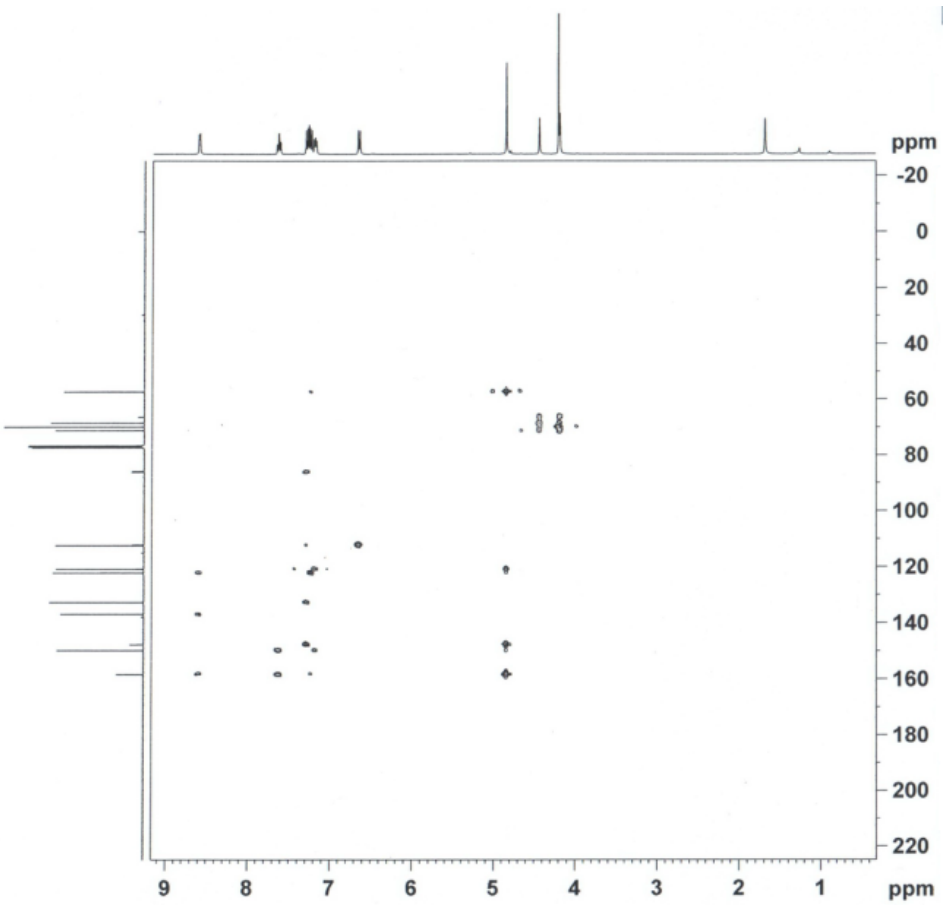

Figure A12 HMBC spectrum of **L2** in CD_3Cl.

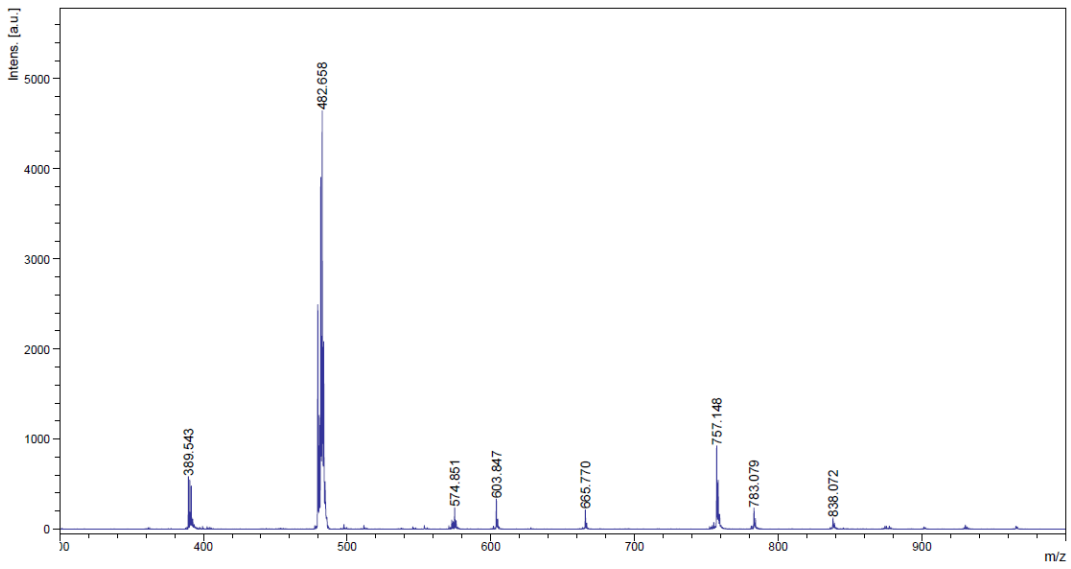

Figure A13 MALDI-TOF mass spectrum of **L2.**

VITA

Miss Orrawan Wisedsoonthorn was born on January 11th, 1992 in Nakhon Phanom province, Thailand. She finished secondary school at Piyamaharachalai school. She graduated and received Bachelor degree from Department of Chemistry, Faculty of Science, Mahasarakham University and completed the program in academic year 2013. Afterward, she was a Master degree student at Chulalongkorn University under supervision of Professor Dr. Thawatchai Tuntulani.